

1 **Modeling study of the 2010 regional haze event in the North**
2 **China Plain**

3

4 **M. Gao^{1,2}, G. R. Carmichael^{1,2}, Y. Wang³, P. E. Saide^{2,a}, M. Yu^{1,2,b}, J. Xin³, Z. Liu³,**
5 **and Z. Wang³**

6 ¹Department of Chemical and Biochemical Engineering, University of Iowa, Iowa City, IA, USA,

7 ²Center for Global and Regional Environmental Research, University of Iowa, Iowa City, IA,
8 USA,

9 ³State Key Laboratory of Atmospheric Boundary Layer Physics and Atmospheric Chemistry,
10 Institute of Atmospheric Physics, Chinese Academy of Sciences, Beijing, China,

11 ^anow at: Atmospheric Chemistry observations and Modeling (ACOM) lab, National Center for
12 Atmospheric Research (NCAR), Boulder, CO, USA

13 ^bnow at: Mathematics and Computer Science Division, Argonne National Laboratory, Argonne,
14 IL, USA

15 Correspondence to: M. Gao and G. R. Carmichael, meng-gao@uiowa.edu;
16 gcarmich@engineering.uiowa.edu

17

18

19

20

21

22

1 **Abstract**

2 The online coupled Weather Research and Forecasting-Chemistry (WRF-Chem) model was
3 applied to simulate a haze event that happened in January 2010 in the North China Plain (NCP),
4 and was validated against various types of measurements. The evaluations indicate that WRF-
5 Chem provides reliable simulations for the 2010 haze event in the NCP. This haze event was
6 mainly caused by high emissions of air pollutants in the NCP and stable weather conditions in
7 winter. Secondary inorganic aerosols also played an important role and cloud chemistry had
8 important contributions. Air pollutants outside Beijing contributed about 64.5% to the PM_{2.5}
9 levels in Beijing during this haze event, and most of them are from south Hebei, Tianjin city,
10 Shandong and Henan provinces. In addition, aerosol feedback has important impacts on surface
11 temperature, Relative Humidity (RH) and wind speeds, and these meteorological variables affect
12 aerosol distribution and formation in turn. In Shijiazhuang, Planetary Boundary Layer (PBL)
13 decreased about 278.2m and PM_{2.5} increased more than 20µg/m³ due to aerosol feedback.
14 Feedbacks associated to Black Carbon (BC) account for about 65.7 % of the PM_{2.5} increases and
15 59.9% of the PBL decreases in Shijiazhuang, indicating more attention should be paid to BC
16 from both air pollution control and climate change perspectives. This contribution decreased
17 from about 60% to 50% after decreasing BC emissions by 50% and the uncertainty can be
18 additionally reduced by improving the model performance in simulating sulfate and OC.

19
20
21
22
23
24
25
26

1 **1 Introduction**

2 The North China Plain (NCP) is one of the most densely populated areas in the world and it has
3 been the Chinese center of culture and politics since early times. Beijing, the capital of China,
4 Tianjin, Shijiazhuang and other big cities with active economic developments are located in the
5 NCP. This region is experiencing heavy haze pollution with record-breaking high concentrations
6 of particulate matters (L. T. Wang et al., 2014). Haze is defined as an air pollution phenomenon
7 where horizontal visibility is less than 10 km caused by aerosol particles, such as dust and Black
8 Carbon (BC), suspended in the atmosphere (Tao et al., 2012). Its formation is highly related to
9 meteorological conditions, emissions of pollutants and gas-to-particle conversion (Sun et al.,
10 2006; Watson, 2002). Haze has attracted much attention for its adverse impacts on visibility and
11 human health. During haze periods, reduced visibility affects land, sea and air traffic safety and
12 the fine particles can directly enter the human body and adhere to lungs to cause respiratory and
13 cardiovascular diseases (Liu et al., 2013). Moreover, haze affects climate and ecosystems via
14 aerosol-cloud-radiation interactions (Sun, et al., 2006; Liu et al., 2013).

15

16 Because haze influences visibility, human health and climate (Gao et al., 2015), numerous
17 studies have used multiple methods to investigate physical, chemical and seasonal characteristics
18 of aerosols during haze. The increase of secondary inorganic aerosols is considered to be an
19 attribute of the haze pollution in east China (Tan et al., 2009; Zhao et al., 2013). Tan et al. (2009)
20 studied the characteristics of aerosols in non-haze and haze days in Guangzhou, China and found
21 that secondary pollutants (OC , SO_4^{2-} , NO_3^- and NH_4^+) were the major components of haze
22 aerosols and they showed a remarkable increase from non-haze to haze days. Similar conclusions
23 were drawn by Zhao et al. (2013) after studying the chemical characteristics of haze aerosols in
24 the NCP. Secondary Organic Aerosol (SOA) formation can also be significant during haze (Tan
25 et al., 2009; Zhao et al., 2013). Studies of aerosol optical properties show that fine-mode aerosols
26 were dominant during haze (Yu et al., 2011; Li et al., 2013). In addition, contributions of diverse
27 factors to haze formation, such as biomass burning and regional transport, have been investigated.
28 Chen et al. (2007) used MM5-CMAQ to reproduce the haze pollution in September 2004 in the
29 Pearl Region Delta (PRD) region and discovered that sea-land breeze played an important role.
30 Wang et al. (2009) discovered that almost 30-90 percent of the organics during the haze

1 happened in June 2007 in Nanjing were from wheat straw burning. Cheng et al. (2014)
2 concluded that biomass burning could cause haze issues and they found biomass burning
3 contributed 37% of PM_{2.5}, 70% of Organic Carbon (OC) and 61% of Elemental Carbon (EC)
4 based upon both modeling and measurement results of case study in summer 2011 in the
5 Yangtze River Delta (YRD) region. These biomass burning events mainly occurred in summer
6 and autumn in east and south China (Cheng et al., 2013, 2014; Li et al., 2010; Wang et al., 2007,
7 2009). To evaluate regional contributors to the haze in southern Hebei, Wang et al. (2012)
8 simulated the time period from 2001 to 2010 and concluded that Shanxi province and the
9 northern Hebei were two major contributors, and winter was the worst season, followed by
10 autumn and summer.

11

12 X. Han et al. (2014) pointed out that the haze formation mechanism in winter in Beijing was
13 different from that in summer and mass concentrations of PM_{2.5} in winter were relatively higher
14 and the compositions were different than in summer. The extreme winter haze in the NCP has
15 attracted enormous scientific interests. It has been found the stagnant meteorological conditions
16 (weak surface wind speed and low Planetary Boundary Layer (PBL) height) and secondary
17 aerosol formation are the main causes of winter haze formation (S. Han et al., 2014; He et al.,
18 2014b; K. Huang et al., 2014; Sun et al., 2014; Wang et al., 2014a; Zhao et al., 2013; Zheng et al.,
19 2014, 2015). Other causes proposed include high local emissions (He et al., 2014b; Zheng et al.,
20 2014), enhanced coal combustion in winter (K. Huang et al., 2014; Sun et al., 2014),
21 heterogeneous chemistry (He et al., 2014a; X. Huang et al., 2014; Quan et al., 2014; Wang et al.,
22 2014a, b; Zheng et al., 2014, 2015) and regional transport (Tao et al., 2014; Sun et al., 2014; L. T.
23 Wang et al., 2014; Z. Wang et al., 2014; Zheng et al., 2014). It was also pointed out that fog
24 processing (K. Huang et al., 2014), aerosol-radiation interactions (J. Wang et al., 2014; Z. Wang
25 et al., 2014; B. Zhang et al., 2015) and nucleation events (Guo et al., 2014) may play important
26 roles in winter haze formation.

27

28 The complex haze formation mechanisms need further studies. Li et al. (2015) emphasized that
29 regional transport of PM_{2.5} is a major cause of severe haze in Beijing, but R. Zhang et al. (2015)
30 pointed out that the evidence provided by Li et al. (2015) is insufficient and regional transport

1 should be evaluated using chemical transport models. Furthermore, the contribution of aerosol
2 feedbacks to $PM_{2.5}$ levels remains unquantified. Therefore, the roles of regional transport and
3 aerosol-radiation interactions in haze events need to be better understood. In this study, the
4 online coupled model WRF-Chem, which is capable of simulating aerosols' effects on
5 meteorology and climate, is used to reproduce the severe haze event that happened in the NCP
6 from 16 to 19 January 2010. During this haze event, the highest hourly $PM_{2.5}$ concentration
7 reached 445.6 and 318.1 $\mu\text{g}/\text{m}^3$ in Beijing and Tianjin and the areas with low visibility covered
8 most eastern China regions (Zhao et al., 2013). In this study, we address the following important
9 questions: (1) what is the performance of the model configurations in representing the
10 meteorological variables, and the physical and chemical characteristics of the aerosols during the
11 selected study period?; (2) How does the haze build up and dissipate?; (3) How do the chemical
12 species of $PM_{2.5}$ change during haze period?; (4) Does regional transport play an import role in
13 the 2010 haze event in Beijing?; (5) What is the contribution of aerosol feedback mechanisms to
14 $PM_{2.5}$ levels during the haze event?; and (6) What is the role of BC absorption in the feedback
15 mechanism? In Sect. 2, we describe the model we use and model configuration, including
16 emissions and used parameterization schemes. In Sect. 3, surface meteorological, chemical
17 observations, atmospheric sounding products, as well as remote sensing products are used to
18 evaluate the model performance. In Sect. 4, questions from (2) to (6) are answered in detail.
19 Conclusions are provided in the Sect. 5.

20

21 **2 Model description and configuration**

22 The WRF-Chem model version 3.5.1 was employed to simulate the 2010 haze event in the NCP
23 region and aerosol-radiation interactions were included (Chapman et al., 2008; Fast et al., 2006).
24 Domain settings are the same as those of Jing-Jin-Ji modeled area of Yu et al. (2012). Three
25 domains with two-way nesting were used and grid resolutions were 81km \times 81km (domain 1),
26 27km \times 27km (domain 2) and 9km \times 9km (domain 3) (see supporting information Figure S1).
27 The number of vertical grids used was 27 and the number of horizontal grids was 81 \times 57, 49 \times 49,
28 and 55 \times 55, respectively. The first domain covers most areas of the East Asia region, including
29 China, Korea, Japan and Mongolia. Beijing was set to be the center of the innermost nested
30 domain. The chemical and aerosol mechanism used was gas-phase chemical mechanism CBMZ

1 (Zaveri and Peters, 1999) coupled with the 8-bin sectional MOSAIC model with aqueous
2 chemistry (Zaveri et al., 2008). MOSAIC treats all the important aerosol species, including
3 sulfate, nitrate, chloride, ammonium, sodium, BC, primary organic mass, liquid water and other
4 inorganic mass (Zaveri et al., 2008). Some of the physics configuration options include Lin
5 cloud-microphysics (Lin et al., 1983), RRTM long wave radiation (Mlawer et al., 1997),
6 Goddard short wave radiation (Chou et al., 1998), Noah land surface model, and the Yonsei
7 University planetary boundary layer parameterization (Hong et al., 2006).

8

9 Emissions are key factors in the accuracy of air quality modeling results. The monthly 2010
10 Multi-resolution Emission Inventory for China (MEIC) (<http://www.meicmodel.org/>) was used
11 as the anthropogenic emissions. This inventory includes emissions of sulfur dioxide (SO₂),
12 nitrogen oxides (NO_x), Carbon Monoxide (CO), non-methane volatile organic compounds
13 (NMVOC), NH₃, BC, organic carbon (OC), PM_{2.5}, PM₁₀, and carbon dioxide (CO₂) by several
14 sectors (power generation, industry, residential, transportation, etc.). Biogenic emissions were
15 calculated on an online way by the MEGAN model (Guenther et al., 2006). Meteorological
16 initial and boundary conditions were obtained from the National Centers for Environmental
17 Prediction (NCEP) Final Analysis (FNL) data set. Chemical initial and boundary conditions were
18 taken from MOZART-4 forecasts (Emmons et al., 2010). The period from 11 to 24 January 2010
19 was chosen as the modeling period, covering the 2010 NCP haze period (from 16 to 19 January
20 2010). To overcome the impacts of initial conditions, three days were simulated and considered
21 as spin-up time.

22

23 **3 Model Evaluation**

24 **3.1 Observation data sets and evaluation metrics**

25 Model evaluation was conducted in terms of both temporal variation and spatial distribution.
26 Table 1 gives a summary of the observation data and variables used in the model evaluation. The
27 meteorological variables, including 2 meter temperature (T2), 2 meter relative humidity (RH2)
28 and 10 meter wind speed (WS10), at four stations (Beijing, Tianjin, Baoding and Chengde) were

1 used. Surface concentrations of PM_{2.5}, NO₂, SO₂ at three sites (Beijing, Tianjin and Xianghe,
2 shown in Figure S1), and Aerosol Optical Depth (AOD) at four sites (Beijing city, Beijing forest,
3 Baoding city, Cangzhou city) were also used in the evaluation against measurements. PM_{2.5} and
4 AOD are typical variables to represent severity of haze pollution. To evaluate how model
5 performs in simulating horizontal and vertical distributions of meteorological and chemical
6 variables, soundings of temperature and RH at Beijing, and AODs derived from CALIPSO were
7 used in this study. The statistical metrics calculated include correlation coefficient R, mean bias
8 (MB), mean error (ME), the root mean square error (RMSE), the normalized mean bias (NMB),
9 the normalized mean error (NME), the mean fractional bias (MFB) and the mean fractional error
10 (MFE). The definitions of these metrics can be found in Morris et al. (2005) and Willmott and
11 Matsuura (2005).

12

13 **3.2 Meteorology simulations**

14 Figure 1 shows the temporal variations of simulated and observed 24-h average temperature (a-
15 d), relative humidity (e-h) and wind speed (i-l) at Beijing, Tianjin, Baoding and Chengde stations.
16 These observations were collected from the China Meteorological Data Sharing Service System
17 (CMDSSS) data set. From normal days to haze days (gray shaded), temperature and relative
18 humidity increased and wind speeds decreased. Generally, the variations of surface temperature,
19 RH and wind speeds are captured by model, although overestimations of wind speed occur at the
20 Chengde station throughout the whole period. Model mean, observation mean, MB, ME and
21 RMSE were calculated and summarized in Table 2. The MB and RMSE for surface temperature
22 vary from -2.0 to 2.0 K and from 1.5 to 3.2 K, respectively. The model underestimates
23 temperature at Beijing, Tianjin and Baoding stations, and overestimates temperature at the
24 Chengde station. RH agrees well with observations, with MB varying from -4.4% to 8.1% and
25 RMSE varying from 6.4% to 11.1%. The magnitudes of MB and RMSE are comparable with
26 those of Wang et al. (2014b). The model shows good performance in simulating wind speed,
27 with RMSE ranging from 1.1 to 1.6 m/s at Beijing, Tianjin and Baoding stations, below the level
28 of “good” model performance criteria for wind speed prediction proposed by Emery et al. (2001).
29 Wind speeds at the Chengde station were overestimated, with RMSE larger than the proposed
30 criteria (2m/s).

1

2 Figure 2 compares simulated and observed vertical temperature profiles at 0800 and 2000 (CST)
3 from January 15 to January 20 at Beijing city. These atmospheric sounding data are from the
4 NCAR Earth observing laboratory atmospheric sounding data set. The model captures the
5 vertical profiles of temperature well. Obvious strong temperature inversions existed during the
6 haze period (from 01/16 08:00 to 01/19 20:00) and the lapse rate during this period was about 5-
7 15°C/km, indicating unfavorable conditions for diffusion of pollutants. The model captures the
8 general vertical profiles of RH, although the performance is not as good as for temperature (see
9 supporting information Figure S2).

10

11 **3.3 Chemical simulations**

12 Figure 3(d-f) shows variations of simulated and observed hourly PM_{2.5}, NO₂ and CO at the SDZ
13 station. The haze event started from 16 January with rapid increase of PM_{2.5}, NO₂, and CO
14 concentrations and ended on 20 January. The relationships between meteorological condition and
15 pollution levels are clearly shown. Both the observation and the model show that temperature
16 and relative humidity increase, wind speeds are low, and pollution levels build up (Figure 3). The
17 magnitudes and trends over time of the simulated PM_{2.5}, NO₂ and CO are generally consistent
18 with measurements, although overestimation of PM_{2.5} and underestimations of NO₂ and CO exist
19 during the haze days. Figure 4 shows the temporal variations of the simulated and observed
20 PM_{2.5}, NO₂ and SO₂ at Beijing (a-c), Tianjin (d-f) and Xianghe (g-i) stations. The observations
21 and the model predictions show that the buildups of pollution during the haze event were similar
22 at these three sites, occurring over a large geographical region at the same time. SO₂ was
23 overestimated in Beijing, but other simulations agree well with observations, especially for PM_{2.5}.
24 Observation mean, model mean, MB, ME, NMB, NME, MFB, and MFE were calculated for 24-
25 h average simulated and observed PM_{2.5} at these three stations and summarized in Table 3. As
26 shown in Table 3, the model underestimates PM_{2.5} concentrations at all stations. NMBs for PM_{2.5}
27 are -8.5%, -26.9% and -39.1% at Beijing, Tianjin and Xianghe, respectively. MFBs at these three
28 stations range from -21.8% to 0.4% and MFEs range from 26.3% to 50.7%. They are all within
29 the criteria proposed by Boylan et al. (2006) that model performance is “satisfactory” when MFB
30 is within ±60% and MFE is below 75%. Although the model performance for PM_{2.5} is

1 satisfactory, biases still exist, especially during severe haze days. Reasons for the biases might be
2 errors in meteorological variables, large uncertainties of emission inventory, effects of horizontal
3 and vertical resolutions, and incomplete treatments of atmospheric chemistry. Many atmospheric
4 chemistry reactions have been and are being proposed for PM formation in winter haze. For
5 example, He et al. (2014a) proposed that mineral dust and NO_x could promote the formation of
6 sulfate in heavy pollution days. The sensitivity of the simulations to some of these factors will be
7 discussed in future studies.

8

9 **3.4 Simulations of optical properties**

10 In WRF-Chem, aerosol optical properties are calculated at four specific wavelengths, 300nm,
11 400nm, 600nm, and 1000nm, while AOD observations from CSHNET, CALIPSO are not at
12 these four wavelengths. To evaluate model performance of simulating AOD, we derived AOD at
13 observation wavelengths based on Angstrom exponent relation (Schuster et al., 2006). In severe
14 haze days, AOD could not be retrieved, so the observed AOD data in some days are missing.
15 Model agrees very well with the CSHNET AOD observations at all four stations (supporting
16 information Figure S3).

17 CALIPSO retrievals provide vertical curtains of aerosol and clouds. Figure 5 shows paths of the
18 CALIPSO satellite, simulated extinction coefficient and observed plume top, and simulated
19 AOD and CALIPSO retrieved AOD at 532nm at three moments: January 14 12:00(CST) (a-c),
20 January 21 02:00(CST) (d-f), and January 21 12:00(CST) (g-i), respectively. There were no
21 retrievals in the NCP during haze days. Figure 5(a), (d) and (g) show that the CALIPSO satellite
22 passed over the NCP region at these three moments. Simulated extinction coefficient matches
23 observed plume top (Figure 5(b), (e) and (h)), indicating that the model captures the vertical
24 distributions of aerosols. The model also has good performance in simulating AOD at 532nm,
25 although underestimations happen around latitude 36°N (Figure 5(c), (f) and (i)).

26

27 The model is shown to be capable of simulating the major meteorological and chemical
28 evolution of this haze event. As spatial and vertical profiles of the haze period are incomplete or
29 missing in the satellite retrievals and ground stations only provide point estimates, we can use the

1 model to understand the haze spatial, vertical and temporal evolution, as discussed in the
2 following sections.

3

4 **4 Results and Discussions**

5 **4.1 Meteorological conditions and evolution of air pollutants**

6 The evolution of the spatial distributions of the haze event is shown in Figure 6, where the
7 horizontal distributions of $PM_{2.5}$ and wind vectors are plotted every 12 hours from January 14
8 00:00 to January 21 00:00. In the second plot (January 14 12:00), air flows converged at the NCP
9 surface areas, resulting in a small increase of $PM_{2.5}$ concentration. From January 14 00:00 to
10 January 16 00:00, $PM_{2.5}$ concentration over the NCP was generally below $120\mu\text{g}/\text{m}^3$. From
11 January 16 to January 18, Beijing and surrounding areas were controlled by a weak high pressure
12 system (Zhao et al., 2013). During this period, large amounts of emissions in the NCP
13 accumulated and the persistent southerly winds brought some air pollutants northward to Beijing
14 and southern Hebei areas. The weak high pressure system was replaced by a low pressure system
15 that lasted until January 20, and this weather condition was not conducive for dispersion of air
16 pollutants (Zhao et al., 2013). On January 19, the NCP haze was in the worst state, with $PM_{2.5}$
17 concentrations above $350\mu\text{g}/\text{m}^3$ in south NCP. From January 20, strong northerly winds
18 dispersed the accumulated air pollutants and the haze ended.

19

20 To illustrate the vertical structure of the haze, vertical cross sections of $PM_{2.5}$ concentration and
21 clouds are presented in Figure 7. The cross section diagonally cuts the region with the lower left
22 corner of 34N, 110E to the upper corner at 44N, 122E (see supporting information Figure S4).
23 There were two highly polluted points (around latitudes 35 and 39) and they started merging as
24 one from January 18 12:00 (Figure 7). At that time, southerly winds blew air pollutants
25 northwards (Figure 6) and the polluted region was expanded. On January 19, there were fog
26 and/or clouds near the surface and the impacts of fog and/or clouds will be discussed in Sect. 4.2.

27

1 Further details of the evolution of the haze are shown in the temporal variations of $PM_{2.5}$
2 concentrations in Shijiazhuang, Tianjin and Chengde (marked in Figure S1) in Figure 8. All three
3 sites show similar temporal variations. Around noon of January 15, $PM_{2.5}$ concentrations in
4 Shijiazhuang, Chengde and Beijing increased at nearly the same time, labeled by red arrow in
5 Figure 8. Air pollutants started accumulating when the NCP was controlled by the weak and
6 stable weather conditions. Compared to Shijiazhuang and Beijing, the capital city of Hebei
7 province and the capital of China, $PM_{2.5}$ concentrations in Chengde were lower (Figure 8). It was
8 estimated that there are more than 8100 coal-fired boilers and industrial kilns in Shijiazhuang
9 city (Peng et al., 2002), resulting in high intensity of emissions in Shijiazhuang. On January 20,
10 Chengde was the first to show sharp decrease of $PM_{2.5}$ concentrations, followed by Beijing and
11 Shijiazhuang, corresponding to the northerly wind impacts discussed above.

12
13 To better understand the relationships between meteorological factors and pollution levels, time
14 series of different pairs of variables are shown in Figure 9. CO shows very high correlation with
15 $PM_{2.5}$ (Figure 9(a)), which is consistent with the observation and modeling results in Santiago,
16 Chile (Perez et al., 2004; Saide et al., 2011), and shows the large contribution of primary sources
17 (including gaseous precursors) to $PM_{2.5}$. Secondary aerosol formation also plays a role as $PM_{2.5}$
18 peaks on the 19th while CO peaks on the 18th. RH and wind speed are two important factors
19 affecting the concentrations of aerosols. RH has similar variations as $PM_{2.5}$ concentration (shown
20 in Figure 9(a) and 5(b)). The NCP is close to the sea and under the slow southerly flows,
21 temperature and RH increase along with $PM_{2.5}$. During the haze event, RH values were generally
22 above 40% and wind speeds were below 2 m/s (Figure 9(b)). Low wind speed is unfavorable for
23 the dilution of air pollutants and high RH would accelerate the formation of secondary species,
24 such as sulfate and nitrate, to aggravate the pollution level (Sun et al., 2006). NO_x concentrations
25 show similar variations as $PM_{2.5}$, indicating the buildup of concentrations during the wind speed
26 stagnation. Ozone shows lower concentrations during haze event (Figure 9(c)) because high
27 aerosol loadings produce low photochemical activity due to decrease in UV radiation. The
28 concentrations have an inverse relationship with PBL Height (PBLH) as shown in Figure 9(d).
29 Diurnal maximums of PBLHs were mostly below 400m and PBL collapsed at night during the
30 haze event, indicating aerosols were trapped near the surface. On January 21 and 22, PBLHs
31 were between 800 and 1000 meters, which helped diffuse and dilute the air pollutants, resulting

1 in a decrease in concentration. The relationships between these variables are further discussed
2 with respect to the influences of aerosol feedback mechanism in Sect. 4.4.

3
4 Figure 10 shows the temporal variations of vertical profiles of simulated $\text{PM}_{2.5}$ concentration (a),
5 temperature (b), RH (c) and wind speeds (d) at the Beijing site. $\text{PM}_{2.5}$ was accumulated below
6 500m and concentrations reached peak values around January 18 00:00 (Figure 10(a)), when a
7 strong temperature inversion happened over Beijing (Figure 10(b)), which inhibited vertical
8 atmospheric mixing. A strong temperature inversion also happened on January 19 (Figure 10(b)).
9 From January 16 to 19, RH was mostly higher than 50% and reached a peak on the night of
10 January 19 (Figure 10(c)). As a result, air pollutants released into the atmosphere were trapped in
11 the moist atmosphere and accumulated as near surface horizontal winds were very weak (below
12 1.5m/s) during the haze period (Figure 10(d)). As mentioned above, the high RH enhances the
13 formation of secondary species, which will be discussed in the following section.

14

15 **4.2 Evolution of aerosol composition during haze**

16 As shown above, during haze events, aerosols build up due to low mixing heights and low wind
17 speeds. An important question is what is the role of secondary aerosol formation during such
18 events? Previous measurement studies have found that the increase of secondary inorganic
19 pollutants could be considered as a common property of haze pollution in East China (Zhao et al.,
20 2013). The observed and simulated chemical species of $\text{PM}_{2.5}$ in Beijing are shown in Figure
21 11(a) and 11(b), respectively. Observed secondary inorganic aerosols (SIA) (NH_4^+ , SO_4^{2-} , NO_3^-)
22 increased significantly during the haze episode and accounted for 37.7% of $\text{PM}_{2.5}$ mass
23 concentration (Zhao et al., 2013). Primary OC, BC, sulfate, nitrate and ammonium accounted for
24 the major parts of the simulated $\text{PM}_{2.5}$ during haze. Table 4 summarizes the mean concentrations
25 of primary aerosols (primary OC and BC) and SIA (NH_4^+ , SO_4^{2-} , NO_3^-) in non-haze days, and
26 in the most serious haze day. The primary aerosols increased by a factor of 4.0 from non-haze
27 days to haze days. The SIA also increased from non-haze days to haze days, which agrees with
28 the observation (Tan et al., 2009; Zhao et al., 2013). The SIA increased by a factor of 7.6 from
29 non-haze days to haze days. The increasing factors for observed primary aerosols and SIA are

1 2.9 and 6.9, which are close to those factors from simulations. However, the amounts of sulfate
2 are underestimated by WRF-Chem, compared with the observation in Figure 11(a) from Zhao et
3 al. (2013). Tuccella et al. (2012) pointed out that the underestimation of simulated sulfate could
4 be due to the underestimation of SO₂ gas phase oxidation, errors in nighttime boundary layer
5 height predicted by WRF-Chem, and/or the uncertainties in aqueous-phase chemistry. It could
6 also be caused by the missing heterogeneous sulfate formation in current model (He et al., 2014a;
7 Wang et al., 2014d; Zheng et al., 2014a). As discussed earlier, the SO₂ gas phase concentrations
8 at this site were overestimated. Adding reaction pathways to produce sulfate aerosol would
9 improve both the predictions of sulfate (increase) and SO₂ (decrease) (He et al., 2014a; Wang et
10 al., 2014c; Zheng et al., 2014a).

11

12 We investigated the role of aqueous phase chemistry during the haze event. The aqueous phase
13 pathway can reach a level of over 50 µg/m³ around the Beijing area, accounting for a significant
14 part (about 14.3%) of total PM_{2.5} concentration (see supporting information Figure S5). As
15 shown in Figure 7, fog/clouds existed near the surface on January 19 and this corresponds to the
16 PM_{2.5} difference on that day due to aqueous phase pathway. The sulfate production in aqueous
17 phase may be higher than shown in this study after adding missing aqueous-phase reactions. The
18 impacts of heterogeneous reactions on sulfate production will be investigated in future studies.

19 As shown in Figure 11(a) and 7(b), the model underestimates OC. To evaluate the formation of
20 Secondary Organic Aerosol (SOA) during the haze event, the RADM2/MADE-SORGAM model
21 was used. The CBMZ/MOSAIC version used is not capable of simulating SOA formation
22 because CBMZ was hard-wired with a numerical solver in WRF-Chem and thus SOA
23 condensable precursors could not be directly added into it (Zhang et al., 2012). RADM2 is an
24 upgrade of RADM1 and it gives more realistic predictions of H₂O₂ (Stockwell et al., 1990), and
25 Schell et al., (2001) incorporated SOA into the Modal Aerosol Dynamics Model for Europe
26 (MADE) (Ackermann et al., 1998) by means of the Secondary Organic Aerosol Model
27 (SORGAM). SORGAM treats anthropogenic and biogenic aerosol precursors separately and
28 eight SOA compounds are considered, of which four are anthropogenic and the other four are
29 biogenic (Schell et al., 2001). Predicted Anthropogenic SOA (ASOA), biogenic SOA (BSOA)
30 and Primary Organic Aerosol (POA) in Beijing are shown in Figure 11(c). SOA indeed shows a

1 marked increase from non-haze days to haze days, but the amount of SOA is very small
2 compared with POA. The highest SOA concentrations in China are usually found in summer and
3 in Central China (Jiang et al., 2012). In addition, almost all of the simulated SOA are ASOA.
4 Jiang et al. (2012) also concluded that in winter, the fractions of ASOA are larger than 90% in
5 north China. Biogenic emissions are usually controlled by solar radiation and temperature, and
6 solar radiation is weaker and temperature is lower in winter compared with summer. Moreover,
7 the high isoprene, API (α-pinene and other cyclic terpenes with one double bond) and LIM
8 (limonene and other cyclic diene terpenes) emissions are located below 30 °N and in Northeast
9 China (Jiang et al., 2012), not in the NCP, so the SOA concentrations are not high in this winter
10 haze event period in the NCP. As shown in Table 4, the mean SOA concentration in non-haze
11 days is 0.15 μg/m³ and in the most serious haze day is 8.2 μg/m³. The factor increase of SOA from
12 non-haze days to haze day is 8.2, which is lower than that of primary aerosols and much lower
13 than that of SIA. The SOA formation in winter has not been well studied and it might be
14 underestimated by the model as it could have missing pathways to SOA formation. Further work
15 is needed to improve the underestimation of SOA formation in the winter.

16

17 **4.3 Impacts of surrounding areas on haze in Beijing**

18 Previous studies found that both local emissions and regional transport have significant
19 contributions to the high fine particle levels in Beijing (Yang et al., 2011). A sensitivity
20 simulation was conducted to quantify the contributions of surrounding areas to haze in Beijing,
21 when Beijing local emissions were turned off. The ratio of PM_{2.5} in Beijing when Beijing
22 emissions are turned off to PM_{2.5} in Beijing when Beijing emissions are on represents the non-
23 local contributions. It can reach above 80% during haze (see supporting information Figure S6)
24 and the average contribution is about 65% from January 16 to January 19.

25 To figure out the dominant transport paths, FLEXPART-WRF (Stohl et al., 1998; Fast and
26 Easter, 2006) was used to generate 72-hour backward dispersions around the Beijing area. 50000
27 particles were released backwards from a box (1 degree×1 degree×400m), the center of which is
28 Beijing urban area, from January 19 00:00. The number concentrations of particles were plotted
29 at 6 hours before, 12 hours before, 24 hours before and 48 hours before the released time (Figure
30 12). For 12 hours, Beijing was influenced by sources to the south, including sources from south

1 Hebei, Tianjin and Shandong. For 2 days, more sources contributed to the haze buildup in
2 Beijing, including sources from Henan and Inner Mongolia. A number of coal mines are located
3 in Hebei, Shandong and Henan provinces and Inner Mongolia areas have high emissions of
4 primary aerosols.

5

6 **4.4 The impact of aerosol feedback**

7 Aerosols affect weather and climate through many pathways, including reducing downward
8 solar radiation through absorption and scattering (direct effect), changing temperature, wind
9 speed, RH and atmospheric stability due to absorption by absorbing aerosols (semi-direct effect),
10 serving as cloud condensation nuclei (CCN) and thus impacting optical properties of clouds (first
11 indirect effect), and affecting cloud coverage, lifetime of clouds and precipitation (second
12 indirect effect) (Zhang et al., 2010; Forkel et al., 2012). The feedback mechanisms are complex
13 and many aspects of them are not well understood. Although previous studies have investigated
14 aerosol-radiation-meteorology interactions (Y. Zhang et al., 2010; R. Forkel et al., 2012), the
15 studies on short time scale events with high aerosol loadings, such as haze events, are limited.
16 This section focuses on evaluating the impacts of aerosol feedback mechanism on meteorology
17 and air quality. The feedback discussed in this paper only includes aerosols' direct and semi-
18 direct effects.

19

20 **4.4.1 Impact of feedback on meteorology and PM_{2.5} distribution**

21 Figure 13(a) shows the observed daily maximum surface solar radiation and simulated surface
22 solar radiation for the with feedback (WF) and without feedback (NF) scenarios in Beijing.
23 Simulated daily maximum surface shortwave radiation values for the NF scenario are higher than
24 observations and the overestimations are reduced by implementing aerosol feedback (Figure
25 13(a)). For the NF case, the correlation coefficient R between simulated and observed daily
26 maximum surface shortwave radiation is 0.84 in Beijing; for the WF scenario, the correlation
27 coefficient increased to R=0.93, and the haze reduced the shortwave radiation values by 30 to
28 80%.

1 The changes in radiation have impacts on the environment. Simulated PBLH and $PM_{2.5}$
2 concentration at Shijiazhuang for the WF and NF scenarios are shown in Figure 13(b) and 13(c).
3 In non-haze days, PBLH differences between the two scenarios are negligible due to low aerosol
4 loadings. In haze days, PBLHs in the WF scenario are generally lower (by up to 60%) than in the
5 NF scenario. As shown in Figure 13(c), $PM_{2.5}$ concentration at Shijiazhuang in WF scenario is
6 higher than it in the NF scenario and the difference reaches about $50\mu g/m^3$ on January 19.
7 Aerosols affect PBLHs in two ways: (1) radiation is scattered back to sky and absorbed, and as a
8 result, radiation reaching the surface is reduced (Figure 13(a)) and temperature is lowered; and (2)
9 suspended aerosols like BC absorb radiation to heat the upper PBL (Ding et al., 2013). Both of
10 these ways increase temperature inversion and atmospheric stability, and thus exacerbate $PM_{2.5}$
11 pollution.

12 Figure 14 shows temporal variations of vertical profiles of (a) $PM_{2.5}$ (c) RH (e) temperature (g)
13 wind speeds differences in Beijing between WF and NF scenarios. When aerosol feedback is
14 included, $PM_{2.5}$ concentrations near Beijing surface are mostly increased, except on the morning
15 of January 17, on the afternoon of January 18 and on January 19 (Figure 14(a)). The increases of
16 $PM_{2.5}$ are caused by the above mentioned decrease of temperature gradient from surface to aloft
17 (shown in Figure 14(e)) and atmospheric stability. Apart from these, $PM_{2.5}$ concentrations are
18 also affected by RH and wind speeds. In WF scenario, RH is generally increased near the surface,
19 especially on January 19 (Figure 14(c)), while horizontal wind speeds are also increased on
20 January 19, which is the main cause of decreases of $PM_{2.5}$ concentrations in Beijing.

21
22 To evaluate the impact of aerosol feedback on horizontal meteorological fields and $PM_{2.5}$
23 distributions, averaged differences of $PM_{2.5}$ concentrations, temperature, PBLHs and horizontal
24 winds between WF and NF scenarios at 2p.m. and 2a.m. in haze days (from January 16 to 19)
25 were calculated and are shown in Figure 15. Figure 15(c) shows that PBLHs are reduced in
26 almost all NCP areas when aerosol feedbacks are considered at 2p.m.. At 2p.m., $PM_{2.5}$
27 concentrations increase about $21.9\mu g/m^3$ at Shijiazhuang ($114.53^\circ E$, $38.03^\circ N$). In a few locations
28 (the areas to the south of Beijing (Figure 15(a)), PM levels decrease although PBLHs are
29 suppressed in those areas. The decreases of $PM_{2.5}$ concentrations in the areas south of Beijing are
30 due to big horizontal wind changes, shown in Figure 15(g). When aerosol feedback is included,

1 surface temperature decreases in areas where there are high aerosol loadings (Figure 15(e)).
2 Figure 15(d) shows that PBLHs are enhanced in east and southwest NCP areas at 2a.m. with
3 aerosol feedback. Aerosol feedback mechanism at night time is more complex compared to it at
4 day time. At night, there is no incoming shortwave radiation from the sun and major radiation is
5 the long wave radiation emitted from the earth. The presence of clouds and some kinds of
6 aerosols can trap outgoing long wave radiation, and as a result, the surface atmosphere is
7 warmed. Different aerosols show different effects on long wave radiation. Greenhouse gases
8 (GHGs) absorb long wave radiation, while large particles like dust scatter long wave radiation.
9 As a result, the upper atmosphere temperature is likely to be warmer or cooler than surface
10 atmosphere temperature. If the upper atmosphere is warmer than the surface, a stable PBL will
11 form. This can explain why aerosol feedbacks increase PBL heights in some regions and
12 decrease in some other regions of NCP. Changes of $PM_{2.5}$ concentrations at 2a.m. are mainly
13 caused by changed PBLHs (Figure 15(b)), showing decreasing trends in areas where PBLHs are
14 enhanced, because changes of winds are relatively small (Figure 15(h)). Temperature changes at
15 2a.m. are similar to it at 2p.m., but the magnitudes are smaller.

16

17 **4.4.2 Impact of BC absorption on meteorology and $PM_{2.5}$ distribution**

18 To investigate BC's influence on meteorology and air quality, sensitivity tests were conducted by
19 removing BC absorption in WRF-Chem (i.e., imaginary refractive index set to zero). Figure 14
20 shows temporal variations of vertical profiles of (b) $PM_{2.5}$ (d) RH (f) temperature and (h) wind
21 speeds differences in Beijing between WF and NBCA scenarios. The differences between WF
22 and NBCA can be used to represent impacts of BC absorption since in WF scenario both
23 scattering and absorbing are considered while in the NBCA scenario only scattering is
24 considered. It is obvious from Figure 14(f) that the upper atmosphere is heated by BC, especially
25 at 1.5km, which increases temperature inversion and atmospheric stability. BC absorption's
26 impacts on $PM_{2.5}$, RH and wind speeds are similar to the impacts of both scattering and
27 absorption, but the magnitudes are smaller (Figure 14(b), (d) and (g)).

28 Figure 16 is similar to Figure 15 except that the differences are between WF and NBCA
29 scenarios. At 2p.m., $PM_{2.5}$ concentration is increased about $14.4\mu\text{g}/\text{m}^3$ in Shijiazhuang (114.53°E ,
30 38.03°N), accounting for about 65.7% of $PM_{2.5}$ changes due to the total aerosol feedback (Figure

1 16(a)). At 2p.m., the maximum decrease in PBLH is about 166.6m (Figure 16(c)), accounting for
2 about 59.9% of the maximum decrease in PBLH in Figure 15(c). At 2p.m., surface temperature
3 in high aerosol loading areas are decreased about 0-2 °C (Figure 16(e)), while the temperature
4 decreases in the same areas are above 2°C in Figure 16(e). At 2a.m., changes of PM_{2.5}, PBLHs,
5 surface temperature and wind speeds are similar to Figure 15, with smaller magnitudes.

6

7 The contribution of BC absorption in aerosol feedbacks depends on the model performance in
8 simulating BC and scattering aerosols (sulfate, OC). As shown in Figure 11, BC was
9 overestimated, and sulfate and OC were underestimated in Beijing. The overestimation could be
10 as large as a factor by 2 in some days. As a result, the relative contributions of BC absorption in
11 aerosol feedbacks are uncertain. To explore the uncertainties of the BC absorption contribution,
12 we conducted a simulation by reducing BC emissions by 50%. The changes of PBLH and PM_{2.5}
13 concentrations at 2p.m. due to aerosol feedbacks and BC absorption after BC emission changes
14 are shown in Figure 17. The domain maximum increases of PM_{2.5} concentrations because of
15 aerosol feedbacks and BC absorption are 19.1μg/m³ and 10.2μg/m³, respectively for the base and
16 50% BC emission cases. The domain maximum decreases of PBLH due to aerosol feedbacks and
17 BC absorption are 235.7m and 114.2m, respectively. These numbers are smaller than before
18 because BC emissions were reduced by 50%. Due to 50% perturbation in BC emissions, the
19 contribution of BC absorption in aerosol feedbacks decreased from about 60% to 50%. This
20 number can be additionally reduced if OC and sulfate concentrations are simulated well. In the
21 future, we can get more accurate estimations of BC absorption in aerosol feedbacks after the
22 performances of simulating BC, OC and sulfate are improved.

23

24 **5 Conclusions**

25 In this study, the online coupled WRF-Chem model was used to reproduce the haze event
26 happened in January, 2010 in the NCP. The model was evaluated against multiple observations,
27 including surface observations of meteorological variables and air pollutants, atmospheric
28 sounding products, surface AOD measurements, and satellite AOD measurements. The
29 correlation coefficients between simulated and observed PM_{2.5} concentrations in Beijing, Tianjin

1 and Xianghe stations are 0.77, 0.75 and 0.69, indicating that WRF-Chem provides reliable
2 representation for the 2010 haze event in the NCP.

3

4 This haze event is mainly caused by high emissions of air pollutants in the NCP region and
5 stable weather conditions in winter. The haze built up almost simultaneously in major cities in
6 the NCP and dissipated from north to south. During haze days, horizontal wind speeds and
7 mixing heights were low, temperature inversion happened above surface and RH values were
8 above 40%. Photochemistry was not significant during haze days due to weak UV radiation. In
9 addition, secondary inorganic aerosols played an important role in the haze event. The role of
10 cloud chemistry in this haze event cannot be ignored.

11

12 The contribution of non-local sources to $PM_{2.5}$ in Beijing was also studied. The average
13 contribution was about 64.5% in haze days. The FLEXPART model was implemented to
14 investigate the sources of the non-local contributions and results show that air pollutants from
15 south Hebei, Tianjin city, Shandong and Henan provinces are the major contributors to the $PM_{2.5}$
16 in Beijing.

17

18 Impacts of high aerosols in haze days on radiation, boundary layer heights and $PM_{2.5}$ have been
19 demonstrated. When aerosol feedback is considered, simulated surface radiation agrees well with
20 observations. In haze days, aerosol feedback has important impacts on surface temperature, RH
21 and wind speeds, and these meteorological variables affect aerosol distribution and formation in
22 turn. The role of BC in aerosol feedback loop has also been investigated. It can account for about
23 as high as 65.7% of the $PM_{2.5}$ increases, and 59.9% of the PBLH decreases in Shijiazhuang.
24 More attention should be paid to BC from both air pollution control and climate change
25 perspectives. Due to the underestimation of sulfate and OC, and overestimation of BC in the
26 current model, the contribution of BC absorption in aerosol feedbacks may have been
27 overestimated. We decreased the BC emission by 50%, and found that the contribution decreased
28 from about 60% to 50%. The uncertainty of this contribution can be additionally reduced by
29 improving the model performance in simulating sulfate and OC.

1

2 **Acknowledgments**

3 Special thanks are given to Dr. Yuesi Wang, Dr. Jinyuan Xin and their research groups for
4 providing measurements to evaluate model performance. The ground observation was supported
5 by the National Natural Science Foundation of China (41222033; 41375036) and the CAS
6 Strategic Priority Research Program Grant (XDA05100102, XDB05020103). We also would like
7 to thank Dr. Yafang Cheng for her contributions to the development of emission processing
8 model. The NCEP FNL data were available at <http://rda.ucar.edu/datasets/ds083.2/>. The MEIC
9 emission inventory data are obtained from <http://www.meicmodel.org/>. The MOZART-4
10 chemical data are available at <http://www.acd.ucar.edu/wrf-chem/mozart.shtml>. Contact M. Gao
11 (meng-gao@uiowa.edu) or G.R. Carmichael (gcarmich@engineering.uiowa.edu) for data
12 requests.

13

14 **References**

- 15 Ackermann, I. J., Hass, H., Memmesheimer, M., Ebel, A., Binkowski, F. S., and Shankar, U. M.
16 A.: Modal aerosol dynamics model for Europe: development and first applications, *Atmos.*
17 *Environ.*, 32, 2981–2999, 1998.
- 18 Boylan, J. W. and Russell, A. G.: PM and light extinction model performance metrics, goals, and
19 criteria for three-dimensional air quality models, *Atmos. Environ.*, 40, 4946–4959,
20 doi:10.1016/j.atmosenv.2005.09.087, 2006.
- 21 Chapman, E. G., Gustafson, Jr., W. I., Easter, R. C., Barnard, J. C., Ghan, S. J., Pekour, M. S.,
22 and Fast, J. D.: Coupling aerosol-cloud-radiative processes in the WRF-Chem model:
23 investigating the radiative impact of elevated point sources, *Atmos. Chem. Phys. Discuss.*, 8,
24 14765–14817, doi: 10.5194/acpd-8-14765-2008, 2008.
- 25 Chen, X.-L., Feng, Y.-R., Li, J.-N., Lin, W.-S., Fan, S.-J., Wang, A.-Y., Fong, S., and Lin, H.:
26 Numerical simulations on the effect of sea-land breezes on atmospheric haze over the Pearl
27 River Delta Region, *Environ. Model. Assess.*, 14, 351–363, doi:10.1007/s10666-007-9131-5,
28 2007.
- 29 Cheng, Y., Engling, G., He, K.-B., Duan, F.-K., Ma, Y.-L., Du, Z.-Y., Liu, J.-M., Zheng, M., and
30 Weber, R. J.: Biomass burning contribution to Beijing aerosol, *Atmos. Chem. Phys.*, 13,
31 7765–7781, doi:10.5194/acp-13-7765-2013, 2013.
- 32 Cheng, Z., Wang, S., Fu, X., Watson, J. G., Jiang, J., Fu, Q., Chen, C., Xu, B., Yu, J., Chow, J.
33 C., and Hao, J.: Impact of biomass burning on haze pollution in the Yangtze River delta,
34 China: a case study in summer 2011, *Atmos. Chem. Phys.*, 14, 4573–4585, doi:10.5194/acp-
35 14-4573-2014, 2014.

- 1 Chou, M.-D., Suarez, M. J., Ho, C.-H., Yan, M. M.-H. and Lee, K.-T.: Parameterizations for
2 cloud overlapping and shortwave single-scattering properties for use in general circulation and
3 cloud ensemble models, *J. Climate*, 11, 202–214, 1998.
- 4 Csavina, J., Field, J., Félix, O., Corral-Avitia, A. Y., Sáez, A. E., and Betterton, E. A.: Effect of
5 wind speed and relative humidity on atmospheric dust concentrations in semi-arid climates,
6 *Sci. Total Environ.*, 487, 82–90, doi:10.1016/j.scitotenv.2014.03.138, 2014.
- 7 Ding, A. J., Fu, C. B., Yang, X. Q., Sun, J. N., Petäjä, T., Kerminen, V.-M., Wang, T., Xie, Y.,
8 Herrmann, E., Zheng, L. F., Nie, W., Liu, Q., Wei, X. L., and Kulmala, M.: Intense
9 atmospheric pollution modifies weather: a case of mixed biomass burning with fossil fuel
10 combustion pollution in eastern China, *Atmos. Chem. Phys.*, 13, 10545–10554,
11 doi:10.5194/acp-13-10545-2013, 2013.
- 12 Emery, C., Tai, E., and Yarwood, G.: Enhanced meteorological modeling and performance
13 evaluation for two Texas ozone episodes, in: Prepared for the Texas Natural Resource
14 Conservation Commission, ENVIRON International Corporation, Novato, CA, USA, 2001.
- 15 Emmons, L. K., Walters, S., Hess, P. G., Lamarque, J.-F., Pfister, G. G., Fillmore, D., Granier, C.,
16 Guenther, A., Kinnison, D., Laepple, T., Orlando, J., Tie, X., Tyndall, G., Wiedinmyer, C.,
17 Baughcum, S. L., and Kloster, S.: Description and evaluation of the Model for Ozone and
18 Related chemical Tracers, version 4 (MOZART-4), *Geosci. Model Dev.*, 3, 43–67,
19 doi:10.5194/gmd-3-43-2010, 2010.
- 20 Fast, J. D. and Easter, R. C.: A Lagrangian Particle Dispersion Model Compatible with WRF, in
21 7th Annual WRF User’s Workshop, 19–22 June 2006, Boulder, CO, USA, P6.2, available at:
22 [http://www2.mmm.ucar.edu/wrf/users/workshops/WS2006/abstracts/PSession06/P6_02_Fast.](http://www2.mmm.ucar.edu/wrf/users/workshops/WS2006/abstracts/PSession06/P6_02_Fast.pdf)
23 pdf (last access: 1 June 2015), 2006.
- 24 Fast, J. D., Gustafson, W. I., Easter, R. C., Zaveri, R. A., Barnard, J. C., Chapman, E. G., Grell,
25 G. A., and Peckham, S. E.: Evolution of ozone, particulates, and aerosol direct radiative
26 forcing in the vicinity of Houston using a fully coupled meteorology-chemistry-aerosol model,
27 *J. Geophys. Res.-Atmos.*, 111, D21305, doi:10.1029/2005JD006721, 2006.
- 28 Forkel, R., Werhahn, J., Hansen, A. B., McKeen, S., Peckham, S., Grell, G., and Suppan, P.:
29 Effect of aerosol-radiation feedback on regional air quality – a case study with WRF/Chem,
30 *Atmos. Environ.*, 53, 202–211, doi:10.1016/j.atmosenv.2011.10.009, 2012.
- 31 Gao, M., Guttikunda, S. K., Carmichael, G. R., Wang, Y., Liu, Z., Stanier, C. O., Saide, P. E., and
32 Yu, M.: Health impacts and economic losses assessment of the 2013 severe haze event in
33 Beijing area, *Sci. Total Environ.*, 511, 553–561, doi:10.1016/j.scitotenv.2015.01.005, 2015.
- 34 Guenther, A., Karl, T., Harley, P., Wiedinmyer, C., Palmer, P. I., and Geron, C.: Estimates of
35 global terrestrial isoprene emissions using MEGAN (Model of Emissions of Gases and
36 Aerosols from Nature), *Atmos. Chem. Phys.*, 6, 3181–3210, doi:10.5194/acp-6-3181-2006,
37 2006.
- 38 Guo, S., Hu, M., Zamora, M. L., Peng, J., Shang, D., Zheng, J., Du, Z., Wu, Z., Shao, M., Zeng,
39 L., Molina, M. J., and Zhang, R.: Elucidating severe urban haze formation in China, *P. Natl.*
40 *Acad. Sci. USA*, 111, 17373–17378, doi:10.1073/pnas.1419604111, 2014.
- 41 Han, S., Wu, J., Zhang, Y., Cai, Z., Feng, Y., Yao, Q., Li, X., Liu, Y., and Zhang, M.:
42 Characteristics and formation mechanism of a winter haze-fog episode in Tianjin, China,
43 *Atmos. Environ.*, 98, 323–330, doi:10.1016/j.atmosenv.2014.08.078, 2014.

- 1 Han, X., Zhang, M., Gao, J., Wang, S., and Chai, F.: Modeling analysis of the seasonal
2 characteristics of haze formation in Beijing, *Atmos. Chem. Phys.*, 14, 10231–10248,
3 doi:10.5194/acp-14-10231-2014, 2014.
- 4 He, H., Tie, X., Zhang, Q., Liu, X., Gao, Q., Li, X., and Gao, Y.: Analysis of the causes of heavy
5 aerosol pollution in Beijing, China: a case study with the WRF-Chem model, *Particuology*, 20,
6 32–40, doi:10.1016/j.partic.2014.06.004, 2014a.
- 7 He, H., Wang, Y., Ma, Q., Ma, J., Chu, B., Ji, D., Tang, G., Liu, C., Zhang, H., and Hao, J.:
8 Mineral dust and NO_x promote the conversion of SO₂ to sulfate in heavy pollution days, *Sci.*
9 *Rep.*, 4, 4172, doi: 10.1038/srep04172, 2014b.
- 10 Hong, S.-Y., Noh, Y., and Dudhia, J.: A New Vertical Di_fusion Package with an Explicit
11 Treatment of Entrainment Processes, *Mon. Weather Rev.*, 134, 2318–2341, 2006.
- 12 Huang, K., Zhuang, G., Wang, Q., Fu, J. S., Lin, Y., Liu, T., Han, L., and Deng, C.: Extreme haze
13 pollution in Beijing during January 2013: chemical characteristics, formation mechanism and
14 role of fog processing, *Atmos. Chem. Phys. Discuss.*, 14, 7517–7556, doi:10.5194/acpd-14-
15 7517-2014, 2014.
- 16 Huang, X., Song, Y., Zhao, C., Li, M., Zhu, T., Zhang, Q., and Zhang, X.: Pathways of sulfate
17 enhancement by natural and anthropogenic mineral aerosols in China, *J. Geophys. Res.-*
18 *Atmos.*, 119, 14165–14179, doi:10.1002/2014JD022301, 2014.
- 19 Li, P., Yan, R., Yu, S., Wang, S., Liu, W., and Bao, H.: Reinstate regional transport of PM_{2.5} as a
20 major cause of severe haze in Beijing, *P. Natl. Acad. Sci. USA*, 112, E2739–E2740,
21 doi:10.1073/pnas.1502596112, 2015.
- 22 Li, W. J., Shao, L. Y., and Buseck, P. R.: Haze types in Beijing and the influence of agricultural
23 biomass burning, *Atmos. Chem. Phys.*, 10, 8119–8130, doi:10.5194/acp-10-8119-2010, 2010.
- 24 Li, Z., Gu, X., Wang, L., Li, D., Xie, Y., Li, K., Dubovik, O., Schuster, G., Goloub, P., Zhang,
25 Y., Li, L., Ma, Y., and Xu, H.: Aerosol physical and chemical properties retrieved from
26 ground based remote sensing measurements during heavy haze days in Beijing winter, *Atmos.*
27 *Chem. Phys.*, 13, 10171–10183, doi:10.5194/acp-13-10171-2013, 2013.
- 28 Lin Y.-L., Farley, R. D., and Orville, H. D.: Bulk parameterization of the snow field in a cloud
29 model, *J. Clim. Appl. Meteorol.*, 22, 1065–1092, 1983.
- 30 Liu, X. G., Li, J., Qu, Y., Han, T., Hou, L., Gu, J., Chen, C., Yang, Y., Liu, X., Yang, T., Zhang,
31 Y., Tian, H., and Hu, M.: Formation and evolution mechanism of regional haze: a case study
32 in the megacity Beijing, China, *Atmos. Chem. Phys.*, 13, 4501–4514, doi:10.5194/acp-13-
33 4501-2013, 2013.
- 34 Mlawer, E. J., Taubman, S. J., Brown, P. D., Iacono, M. J., and Clough, S. A.: Radiative transfer
35 for inhomogeneous atmospheres: RRTM, a validated correlated-k model for the longwave, *J.*
36 *Geophys. Res.*, 102, 16663–16682, doi:10.1029/97JD00237, 1997.
- 37 Morris, R. E., McNally, D. E., Tesche, T. W., Tonnesen, G., Boylan, J. W., and Brewer, P.:
38 Preliminary evaluation of the community multiscale air quality model for 2002 over the
39 southeastern United States, *J. Air Waste Manage.*, 55, 1694–1708,
40 doi:10.1080/10473289.2005.10464765, 2005.
- 41 Paciorek, C. J., Liu, Y., Moreno-Macias, H., and Kondragunta, S.: Spatiotemporal associations
42 between GOES aerosol optical depth retrievals and ground-level PM_{2.5}, *Environ. Sci.*
43 *Technol.*, 42, 5800–5806, 2008.
- 44 Peng, C., Wu, X., Liu, G., Johnson, T., and Shah, J.: Urban air quality and health in China,
45 *Urban Stud.*, 39, 2283–2299, doi:10.1080/0042098022000033872, 2002.

- 1 Perez, P., Palacios, R., and Castillo, A.: Carbon monoxide concentration forecasting in Santiago,
2 Chile, *J. Air Waste Manage.*, 54, 908–913, doi:10.1080/10473289.2004.10470966, 2004.
- 3 Quan, J., Tie, X., Zhang, Q., Liu, Q., Li, X., Gao, Y., and Zhao, D.: Characteristics of heavy
4 aerosol pollution during the 2012–2013 winter in Beijing, China, *Atmos. Environ.*, 88, 83–89,
5 doi:10.1016/j.atmosenv.2014.01.058, 2014.
- 6 Saide, P. E., Carmichael, G. R., Spak, S. N., Gallardo, L., Osses, A. E., Mena-Carrasco, M. A.,
7 and Pagowski, M.: Forecasting urban PM₁₀ and PM_{2.5} pollution episodes in very stable
8 nocturnal conditions and complex terrain using WRF–Chem CO tracer model, *Atmos.*
9 *Environ.*, 45, 2769–2780, doi:10.1016/j.atmosenv.2011.02.001, 2011.
- 10 Schell, B., Ackermann, I. J., Hass, H., and Carolina, N.: Modeling the formation of secondary
11 organic aerosol within a comprehensive air quality model system, *J. Geophys. Res.*, 106,
12 28275–28293, 2001.
- 13 Schuster, G. L., Dubovik, O., and Holben, B. N.: Angstrom exponent and bimodal aerosol size
14 distributions, *J. Geophys. Res.*, 111, D07207, doi:10.1029/2005JD006328, 2006.
- 15 Stockwell, W. R., Middleton, P., and Chang, J. S.: The second generation regional acid
16 deposition model chemical mechanism for regional air quality modeling, *J. Geophys. Res.*, 95,
17 16343–16367, 1990.
- 18 Stohl, A., Hittenberger, M., and Wotawa, G.: Validation of the lagrangian particle dispersion
19 model FLEXPART against large-scale tracer experiment data, *Atmos. Environ.*, 32, 4245–
20 4264, doi:10.1016/S1352-2310(98)00184-8, 1998.
- 21 Sun, Y., Zhuang, G., Tang, A. A., Wang, Y., and An, Z.: Chemical characteristics of PM_{2.5} and
22 PM₁₀ in haze-fog episodes in Beijing, *Environ. Sci. Technol.*, 40, 3148–3155, 2006.
- 23 Sun, Y., Jiang, Q., Wang, Z., Fu, P., Li, J., Yang, T., and Yin, Y.: Investigation of the sources
24 and evolution processes of severe haze pollution in Beijing in January 2013, *J. Geophys. Res.-*
25 *Atmos.*, 119, 4380–4398, doi:10.1002/2014JD021641, 2014.
- 26 Tan, J.-H., Duan, J.-C., Chen, D.-H., Wang, X.-H., Guo, S.-J., Bi, X.-H., Sheng, G.-Y., He, K.-B.,
27 and Fu, J.-M.: Chemical characteristics of haze during summer and winter in Guangzhou,
28 *Atmos. Res.*, 94, 238–245, doi:10.1016/j.atmosres.2009.05.016, 2009.
- 29 Tao, M., Chen, L., Su, L., and Tao, J.: Satellite observation of regional haze pollution over the
30 North China Plain, *J. Geophys. Res. Atmos.*, 117, D12203, doi:10.1029/2012JD017915, 2012.
- 31 Tao, M., Chen, L., Xiong, X., Zhang, M., Ma, P., Tao, J., and Wang, Z.: Formation process of
32 the widespread extreme haze pollution over northern China in January 2013: Implications for
33 regional air quality and climate, *Atmos. Environ.*, 98, 417–425, 10
34 doi:10.1016/j.atmosenv.2014.09.026, 2014.
- 35 Wang, G., Kawamura, K., Xie, M., Hu, S., Cao, J., An, Z., Waston, J. G., and Chow, J. C.:
36 Organic molecular compositions and size distributions of Chinese summer and autumn
37 aerosols from Nanjing: characteristic haze event caused by wheat straw burning, *Environ. Sci.*
38 *Technol.*, 43, 6493–6499, 2009.
- 39 Wang, J., Wang, S., Jiang, J., Ding, A., Zheng, M., Zhao, B., Wong, D. C., Zhou, W., Zheng,
40 G., Wang, L., Pleim, J. E., and Hao, J.: Impact of aerosol–meteorology interactions on fine
41 particle pollution during China’s severe haze episode in January 2013, *Environ. Res. Lett.*, 9,
42 094002, doi:10.1088/1748-9326/9/9/094002, 2014.
- 43 Wang, L., Xu, J., Yang, J., Zhao, X., Wei, W., Cheng, D., Pan, X., and Su, J.: Understanding haze
44 pollution over the southern Hebei area of China using the CMAQ model, *Atmos. Environ.*, 56,
45 69–79, doi:10.1016/j.atmosenv.2012.04.013, 2012.

- 1 Wang, L. T., Wei, Z., Yang, J., Zhang, Y., Zhang, F. F., Su, J., Meng, C. C., and Zhang, Q.: The
2 2013 severe haze over southern Hebei, China: model evaluation, source apportionment, and
3 policy implications, *Atmos. Chem. Phys.*, 14, 3151–3173, doi:10.5194/acp-14-3151-2014,
4 2014.
- 5 Wang, Q., Shao, M., Liu, Y., William, K., Paul, G., Li, X., Liu, Y., and Lu, S.: Impact of
6 biomass burning on urban air quality estimated by organic tracers: Guangzhou and Beijing as
7 cases, *Atmos. Environ.*, 41, 8380–8390, doi:10.1016/j.atmosenv.2007.06.048, 2007.
- 8 Wang, Y., Yao, L., Wang, L., Liu, Z., Ji, D., Tang, G., Zhang, J., Sun, Y., Hu, B., and Xin, J.:
9 Mechanism for the formation of the January 2013 heavy haze pollution episode over central
10 and eastern China, *Sci. China Earth Sci.*, 57, 14–25, doi:10.1007/s11430-013-4773-4, 2014a.
- 11 Wang, Y., Zhang, Q., Jiang, J., Zhou, W., Wang, B., He, K., Duan, F., Zhang, Q., Philip, S., and
12 Xie, Y.: Enhanced sulfate formation during China's severe winter haze episode in January
13 2013 missing from current models, *J. Geophys. Res.-Atmos.*, 119, 10425–10440,
14 doi:10.1002/2013JD021426, 2014b.
- 15 Wang, Z., Li, J., Wang, Z., Yang, 5 W., Tang, X., Ge, B., Yan, P., Zhu, L., Chen, X., Chen, H.,
16 Wand, W., Li, J., Liu, B., Wang, X., Zhao, Y., Lu, N., and Su, D.: Modeling study of regional
17 severe hazes over mid-eastern China in January 2013 and its implications on pollution
18 prevention and control, *Sci. China Earth Sci.*, 57, 3–13, doi:10.1007/s11430-013-4793-0,
19 2014.
- 20 Watson, J. G.: Visibility: science and regulation, *J. Air Waste Manage. Assoc.*, 52, 628–713, 10
21 doi:10.1080/10473289.2002.10470813, 2002.
- 22 Willmott, C. J. and Matsuura, K.: Advantages of the mean absolute error (MAE) over the root
23 mean square error (RMSE) in assessing average model performance, *Clim. Res.*, 30, 79–82,
24 2005.
- 25 Yang, F., Tan, J., Zhao, Q., Du, Z., He, K., Ma, Y., Duan, F., Chen, G., and Zhao, Q.:
26 Characteristics of PM_{2.5} speciation in representative megacities and across China, *Atmos.*
27 *Chem. Phys.*, 11, 5207–5219, doi:10.5194/acp-11-5207-2011, 2011.
- 28 Yu, M., Carmichael, G. R., Zhu, T., and Cheng, Y.: Sensitivity of predicted pollutant levels to
29 urbanization in China, *Atmos. Environ.*, 60, 544–554, doi:10.1016/j.atmosenv.2012.06.075,
30 2012.
- 31 Yu, X., Zhu, B., Yin, Y., Yang, J., Li, Y., and Bu, X.: A comparative analysis of aerosol
32 properties in dust and haze-fog days in a Chinese urban region, *Atmos. Res.*, 99, 241–247,
33 doi:10.1016/j.atmosres.2010.10.015, 2011.
- 34 Zaveri, R. A., and Peters, L. K.: A new lumped structure photochemical mechanism for large-
35 scale applications, *J. Geophys. Res.*, 104, 30387–30415, doi:10.1029/1999JD900876,25 1999.
- 36 Zaveri, R. A., Easter, R. C., Fast, J. D., and Peters, L. K.: Model for Simulating Aerosol
37 Interactions and Chemistry (MOSAIC), *J. Geophys. Res.*, 113, D13204,
38 doi:10.1029/2007JD008782, 2008.
- 39 Zhang, B., Wang, Y., and Hao, J.: Simulating aerosol–radiation–cloud feedbacks on meteorology
40 and air quality over eastern China under severe haze conditions in winter, *Atmos. Chem. Phys.*,
41 15, 2387–2404, doi:10.5194/acp-15-2387-2015, 2015.
- 42 Zhang, R., Guo, S., Zamora, M. L., and Hu, M.: Reply to Li et al.: Insufficient evidence for the
43 contribution of regional transport to severe haze formation in Beijing, *P. Natl. Acad. Sci. USA*,
44 1, 1073, doi:10.1073/pnas.1503855112, 2015.
- 45

1 Zhang, Y., Wen, X.-Y., and Jang, C. J.: Simulating chemistry–aerosol–cloud–radiation–climate
2 feedbacks over the continental U.S. using the online-coupled Weather Research Forecasting
3 Model with chemistry (WRF/Chem), *Atmos. Environ.*, 44, 3568–3582,
4 doi:10.1016/j.atmosenv.2010.05.056, 2010.

5 Zhang, Y., Chen, Y., Sarwar, G., and Schere, K.: Impact of gas-phase mechanisms on Weather
6 Research Forecasting Model with Chemistry (WRF/Chem) predictions: mechanism
7 implementation and comparative evaluation, *J. Geophys. Res.*, 117, D01301,
8 doi:10.1029/2011JD015775, 2012.

9 Zhao, X. J., Zhao, P. S., Xu, J., Meng, W., Pu, W. W., Dong, F., He, D., and Shi, Q. F.: Analysis
10 of a winter regional haze event and its formation mechanism in the North China Plain, *Atmos.*
11 *Chem. Phys.*, 13, 5685–5696, doi:10.5194/acp-13-5685-2013, 2013.

12 Zheng, B., Zhang, Q., Zhang, Y., He, K. B., Wang, K., Zheng, G. J., Duan, F. K., Ma, Y. L., and
13 Kimoto, T.: Heterogeneous chemistry: a mechanism missing in current models to explain
14 secondary inorganic aerosol formation during the January 2013 haze episode in North China,
15 *Atmos. Chem. Phys.*, 15, 2031–2049, doi:10.5194/acp-15-2031-2015, 2015.

16 Zheng, G. J., Duan, F. K., Ma, Y. L., Cheng, Y., Zheng, B., Zhang, Q., Huang, T., Kimoto, T.,
17 Chang, D., Su, H., Pöschl, U., Cheng, Y. F., and He, K. B.: Exploring the severe winter haze
18 in Beijing, *Atmos. Chem. Phys. Discuss.*, 14, 17907–17942, doi:10.5194/acpd-14-17907-2014,
19 2014.

20

21

22

23

24

25

26

27

28

29

30

31

32

33

Table 1. Observation Data and Variables Used in This Study

Data sets ^a	Variables ^b	Data frequency	Number of sites used	Data sources
CMDSSS	T2, RH2, WS10	Daily	4	http://cdc.cma.gov.cn/home.do
Atmospheric Sounding	T, RH	12 hours	1	http://weather.uwyo.edu/uppe_rair/sounding.html
CARE-China	PM _{2.5} , NO ₂ , SO ₂	Hourly	3	
CSHNET	AOD	Hourly	4	
SDZ	T1.5, RH1.5, WS10, PM _{2.5} , NO ₂ , CO	Hourly	1	Zhao et al. (2013)
CALIPSO	AOD	N/A	N/A	http://www-calipso.larc.nasa.gov/
MODIS	AOD	Daily	N/A	http://ladsweb.nascom.nasa.gov/data/search.html

^aCMDSSS—China Meteorological Data Sharing Service System; CARE-China—Campaign on the atmospheric

Aerosol Research network of China; CSHNET—Chinese Sun Hazemeter Network; SDZ—Observation data at

Shangdianzi site are extracted from paper Zhao et al. (2013); CALIPSO—The Cloud-Aerosol Lidar and Infrared

Pathfinder Satellite Observation; MODIS—the Moderate Resolution Imaging Spectroradiometer. ^bT2— temperature

1 at 2m; RH2—relative humidity at 2m; WS10—wind speed at 10m; T1.5—temperature at 1.5m; RH1.5—relative
 2 humidity at 1.5m; AOD—Aerosol Optical Depth.

3
 4
 5 Table 2. Performance Statistics for Meteorological Variables

6
 Variables

Variables	Beijing					Tianjin					Baoding					Chengde				
	Obs.	Mod.	MB	ME	RMSE	Obs.	Mod.	MB	ME	RMSE	Obs.	Mod.	MB	ME	RMSE	Obs.	Mod.	MB	ME	RMSE
T2(K)	269.5	267.6	-1.9	2.0	2.5	269.3	268.1	-1.1	1.2	1.5	270.4	268.5	-2.0	2.0	2.3	262.5	264.5	2.0	2.4	3.2
RH2 (%)	46.9	53.4	6.6	7.2	11.1	61.5	58.4	-3.1	5.9	6.4	44.4	52.5	8.1	8.1	10.4	59.4	55.0	-4.4	8.0	8.8
WS10(m/s)	2.1	3.4	1.3	1.3	1.6	2.8	3.2	0.4	1.0	1.1	1.4	2.8	1.4	1.4	2.1	1.4	2.9	1.5	1.5	1.8

7
 8
 9 Table 3. Performance Statistics of PM_{2.5}

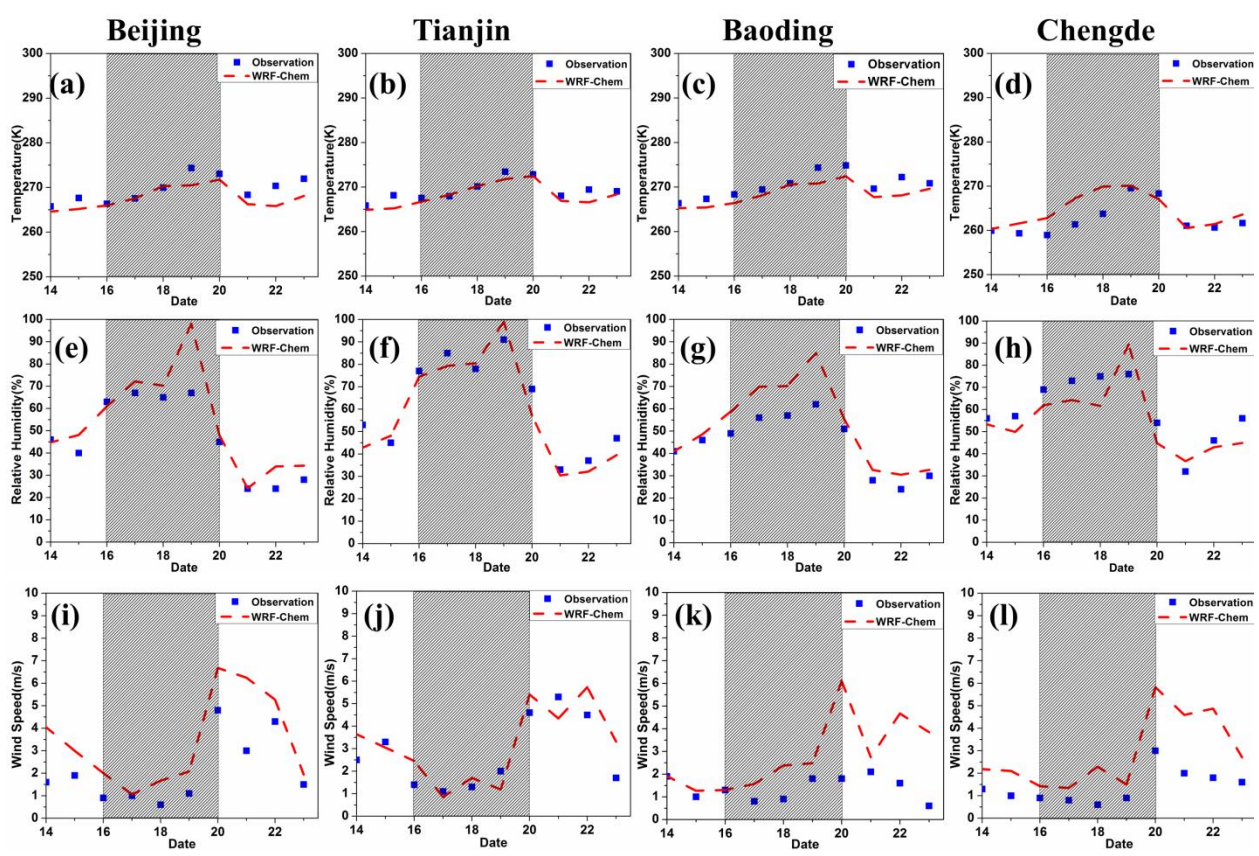
	Obs. ($\mu\text{g}/\text{m}^3$)	Model ($\mu\text{g}/\text{m}^3$)	R	MB ($\mu\text{g}/\text{m}^3$)	ME ($\mu\text{g}/\text{m}^3$)	NMB (%)	NME (%)	MFB (%)	MFE (%)
Beijing	111.7	122.1	0.77	-10.4	30.4	-8.5	24.9	0.4	26.3
Tianjin	103.3	141.2	0.75	-37.9	56.1	-26.9	39.7	-7.8	49.6
Xianghe	93.0	152.6	0.69	-59.7	68.0	-39.1	44.5	-21.8	50.7

10
 11
 12
 13

1 Table 4. Primary Aerosol, SIA and SOA ($\mu\text{g}/\text{m}^3$) during Haze Days and Non-haze Days in
 2 Beijing

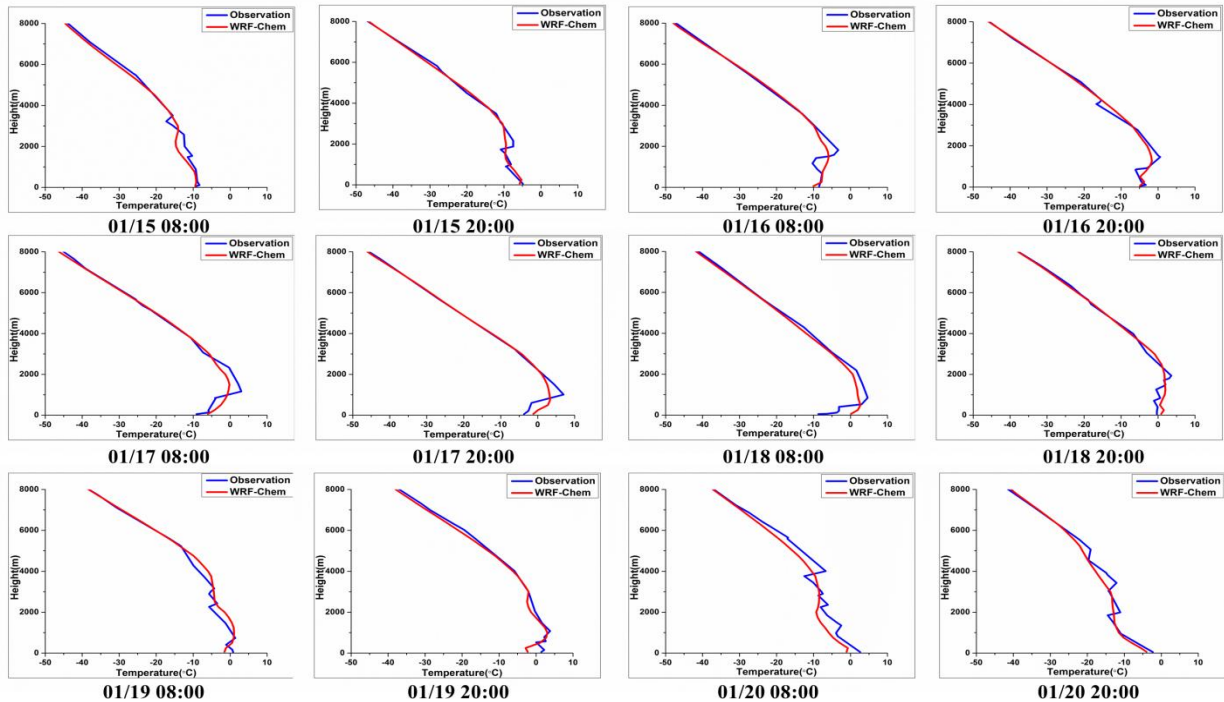
	Primary	SIA	SOA
Haze days	56.4	81.9	1.1
Non-haze days	14.2	10.8	0.3
Ratio	4.0	7.6	3.7

3
4

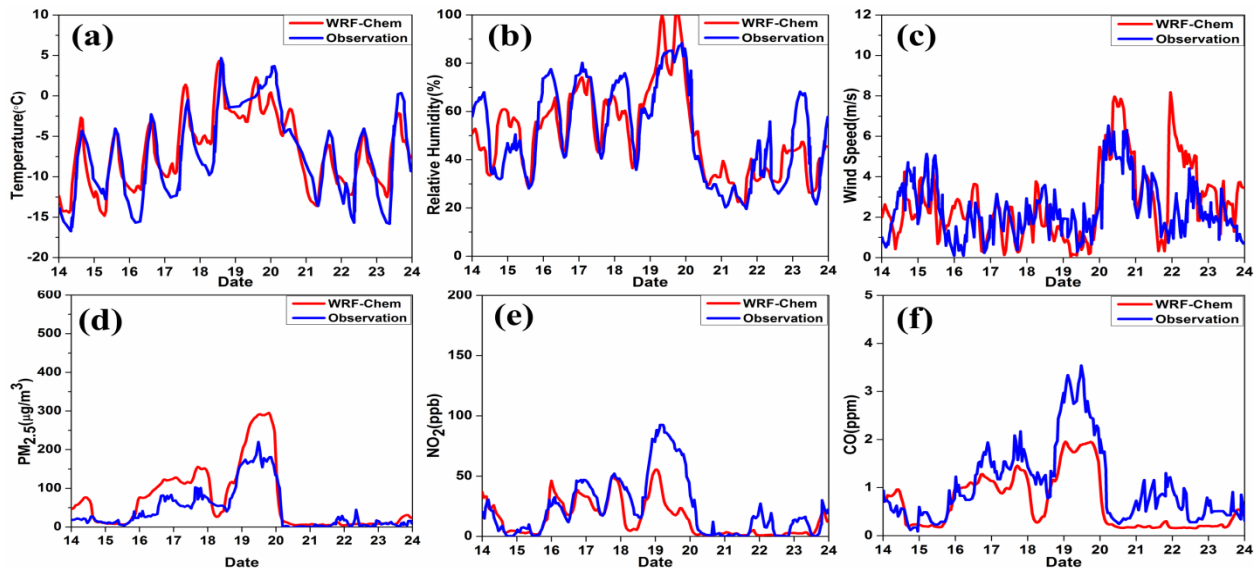


5

6 Figure 1. The temporal variations of observed and simulated 24-h average temperature (a-d),
 7 relative humidity (e-h) and wind speed (i-l) in the Beijing, Tianjin, Baoding, and Chengde
 8 stations

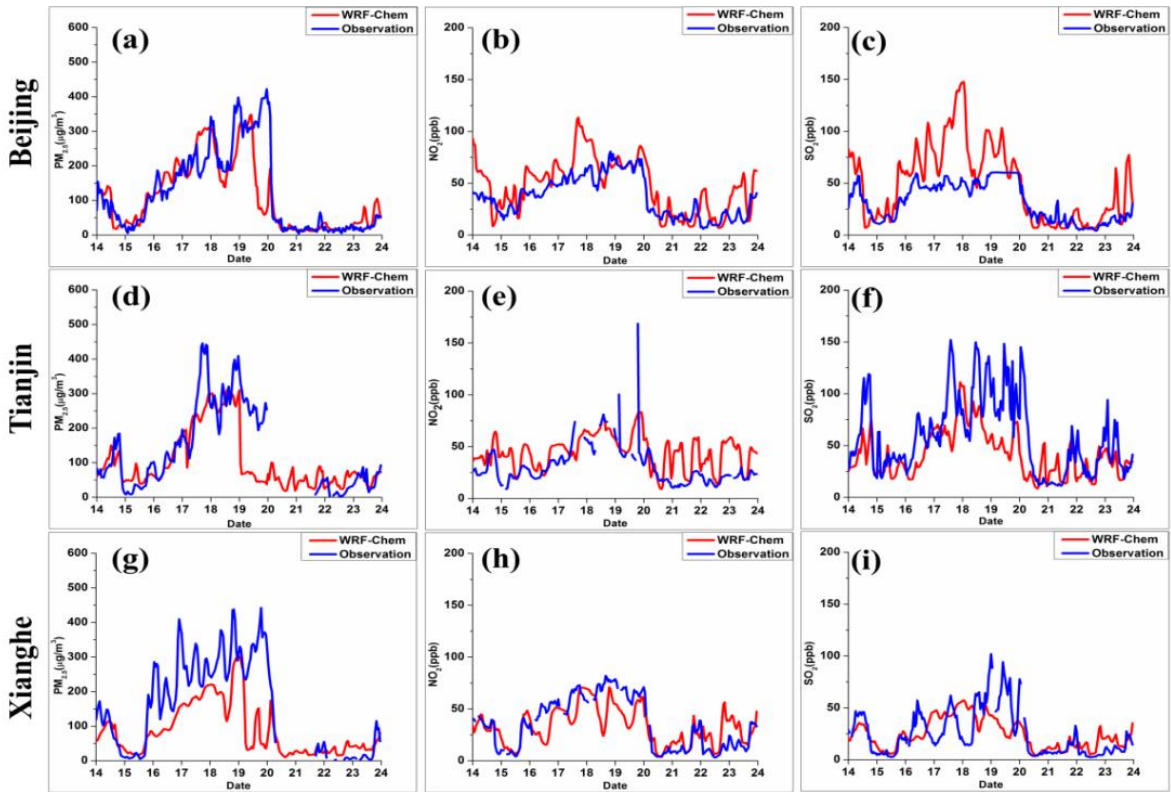


1
 2 Figure 2. Simulated and observed vertical temperature profiles at 0800 and 2000 (China Standard
 3 Time, CST) from 15 January to 20 January
 4



5
 6 Figure 3. Simulated and observed hourly temperature, RH, wind speed, PM_{2.5}, NO₂ and CO in
 7 the Shangdianzi (SDZ) station

1



2

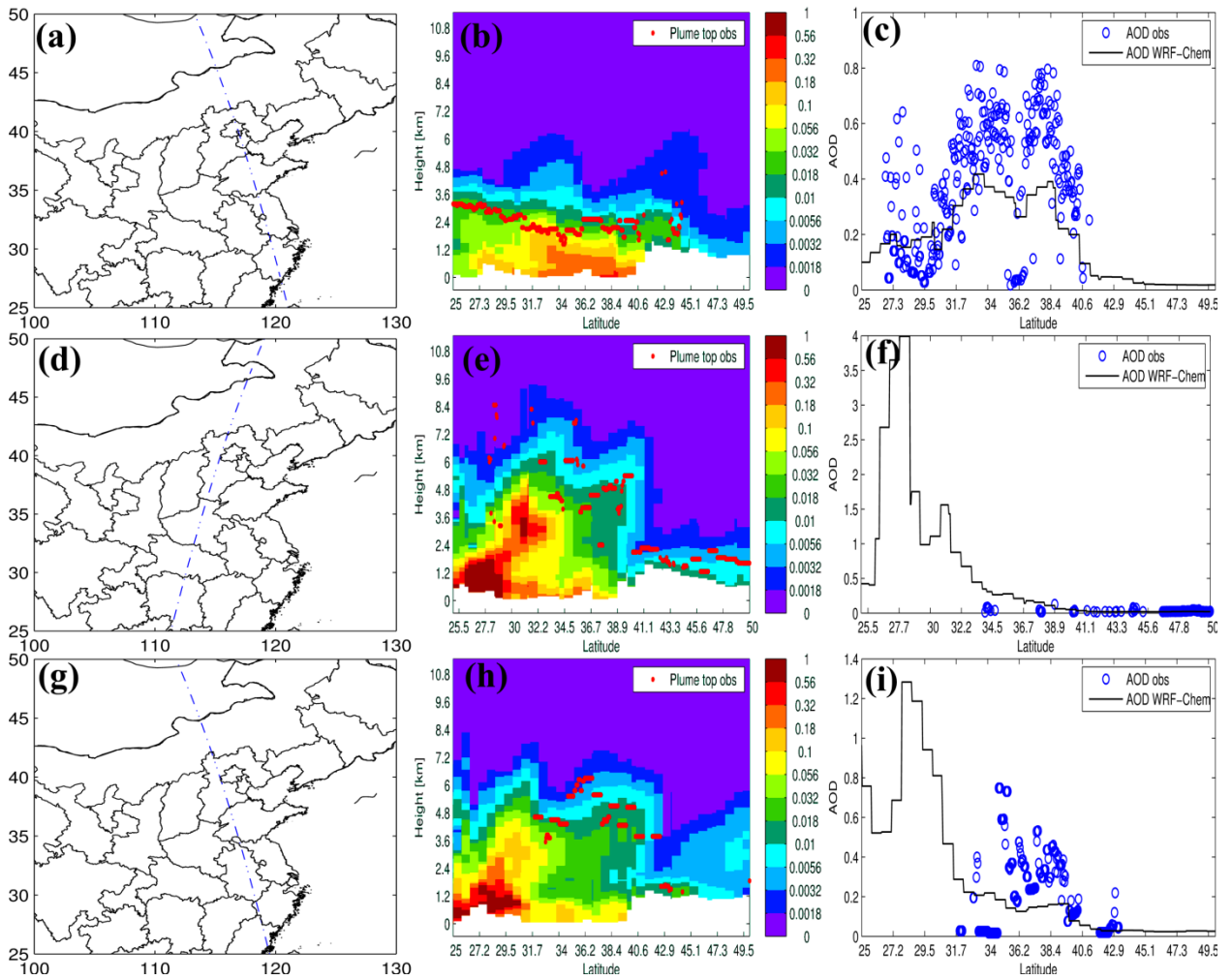
3 Figure 4. Temporal variations of the simulated and observed $PM_{2.5}$, NO_2 and SO_2 at Beijing (a-c),

4

5 Tianjin (d-f) and Xianghe (g-i) stations

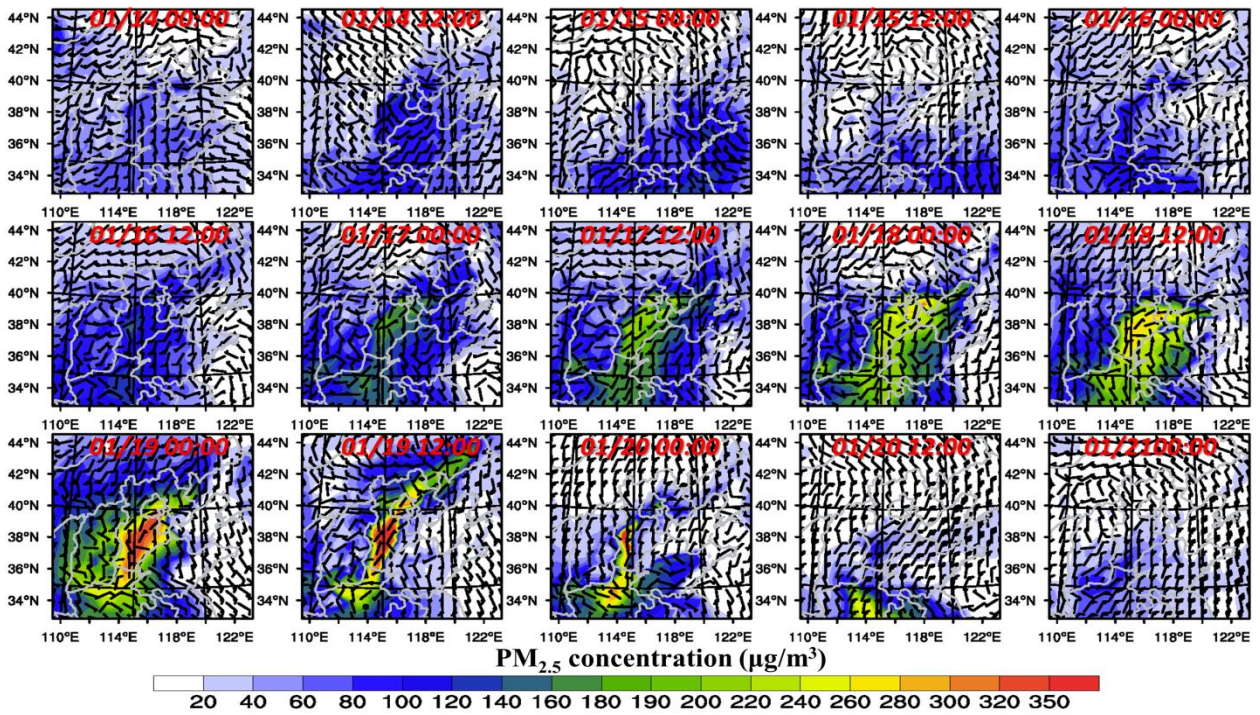
6

7

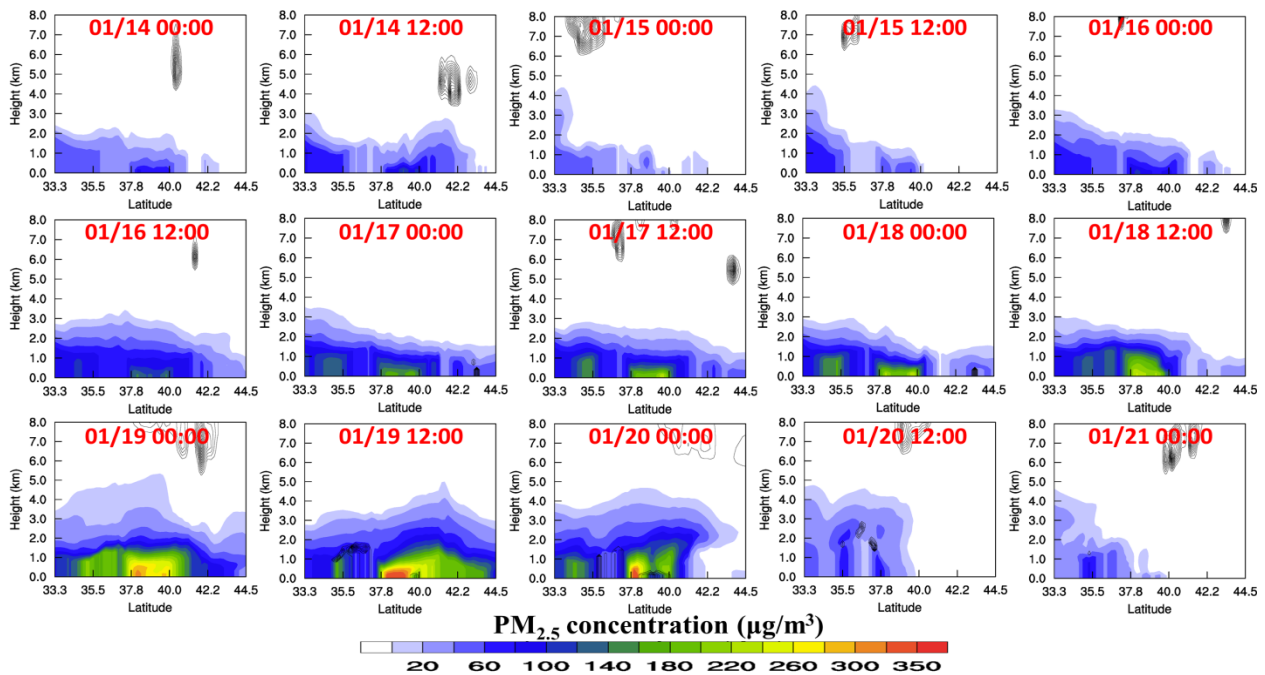


1
2
3
4
5
6

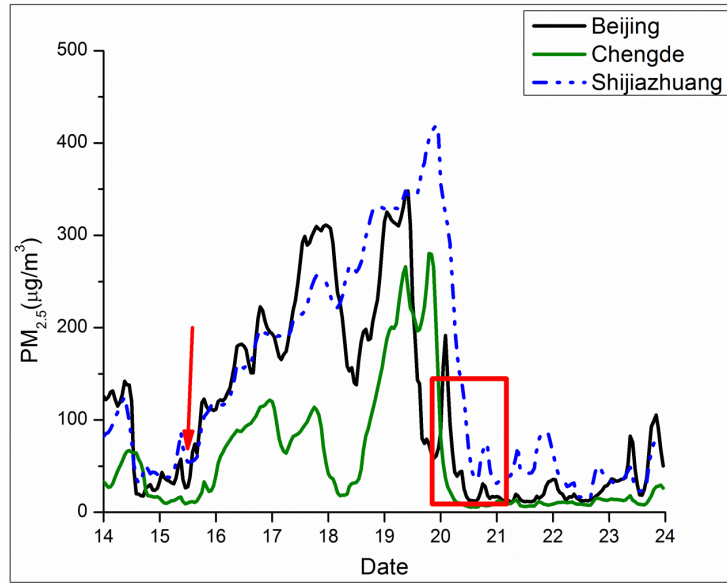
Figure 5. Routes of CALIPSO satellite, simulated extinction coefficient and observed plume top, and simulated AOD and CALIPSO retrieved AOD at 532nm at three moments: January 14 12:00(CST) (a-c), January 21 02:00(CST) (d-f), and January 21 12:00(CST) (g-i)



1
 2 Figure 6. PM_{2.5} concentration from 14 January 00:00 to 21 00:00 January, plotted every 12 hours



3
 4
 5 Figure 7. Cross section plots of PM_{2.5} concentration and clouds from 14 January 00:00 to 21
 6 00:00 January every 12 hours

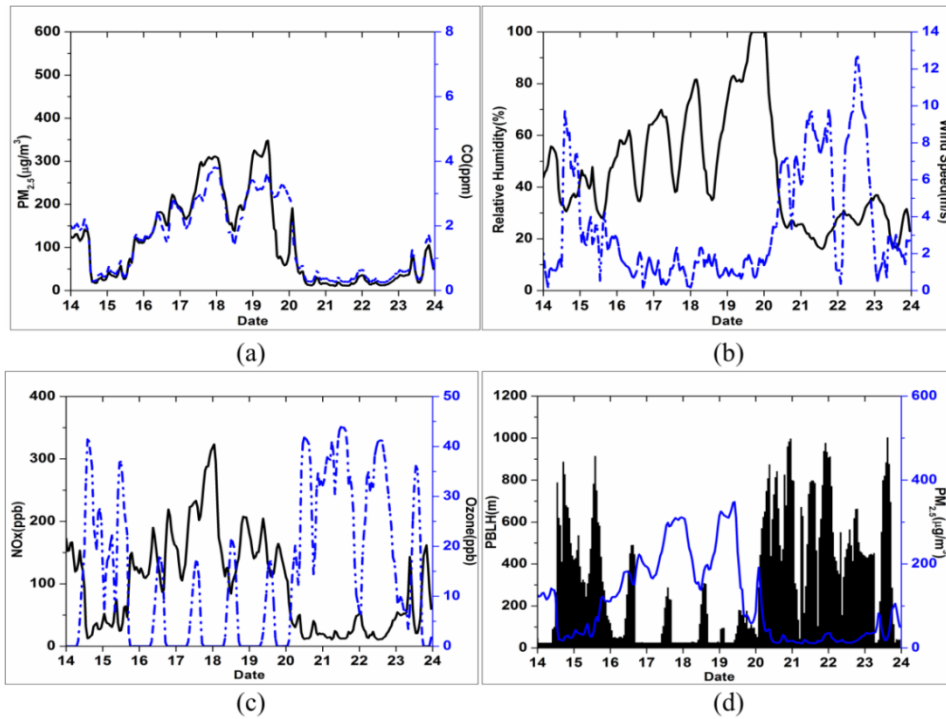


1

2

Figure 8. Temporal variations of simulated $PM_{2.5}$ at Shijiazhuang, Beijing and Chengde

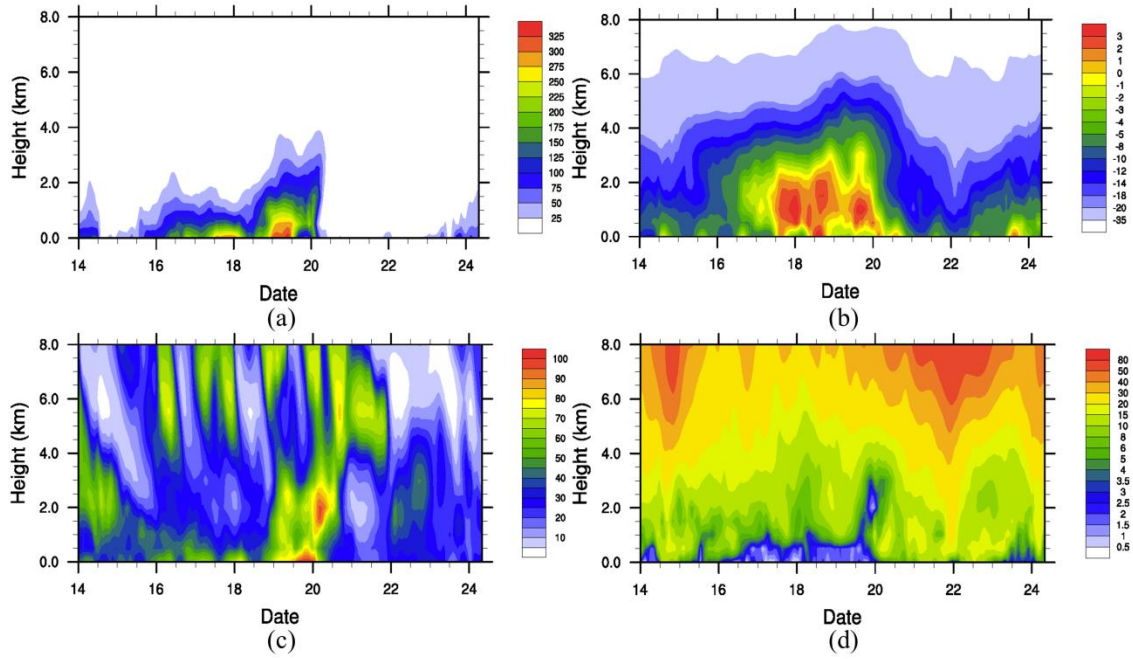
3



4

5

Figure 9. Simulated temporal variations of meteorological and chemical variables in Beijing



1

2

3

4

Figure 10. Temporal variations of vertical profiles of simulated (a) PM_{2.5} (unit: μg/m³) (b) temperature (unit: °C) (c) RH (unit: %) (d) wind speeds (unit: m/s) in Beijing

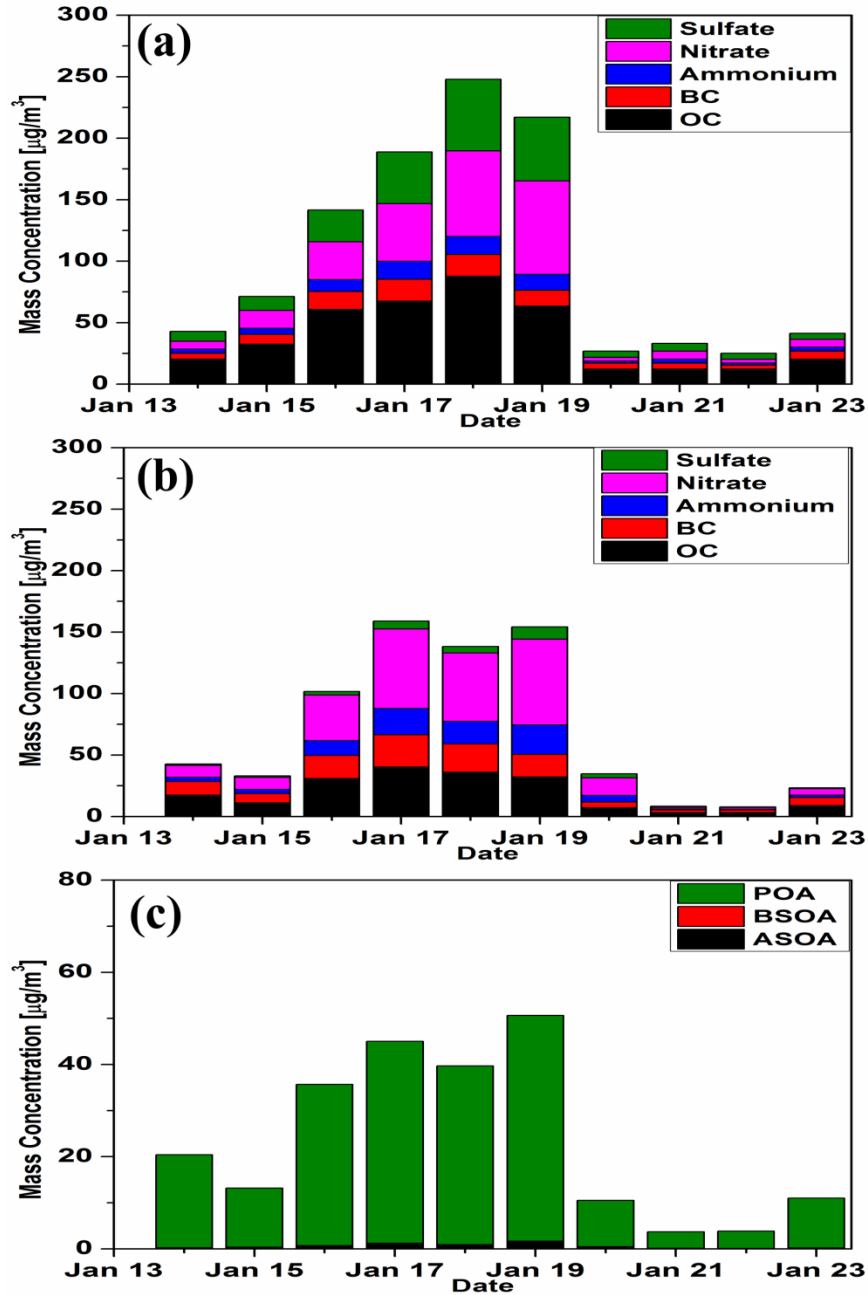
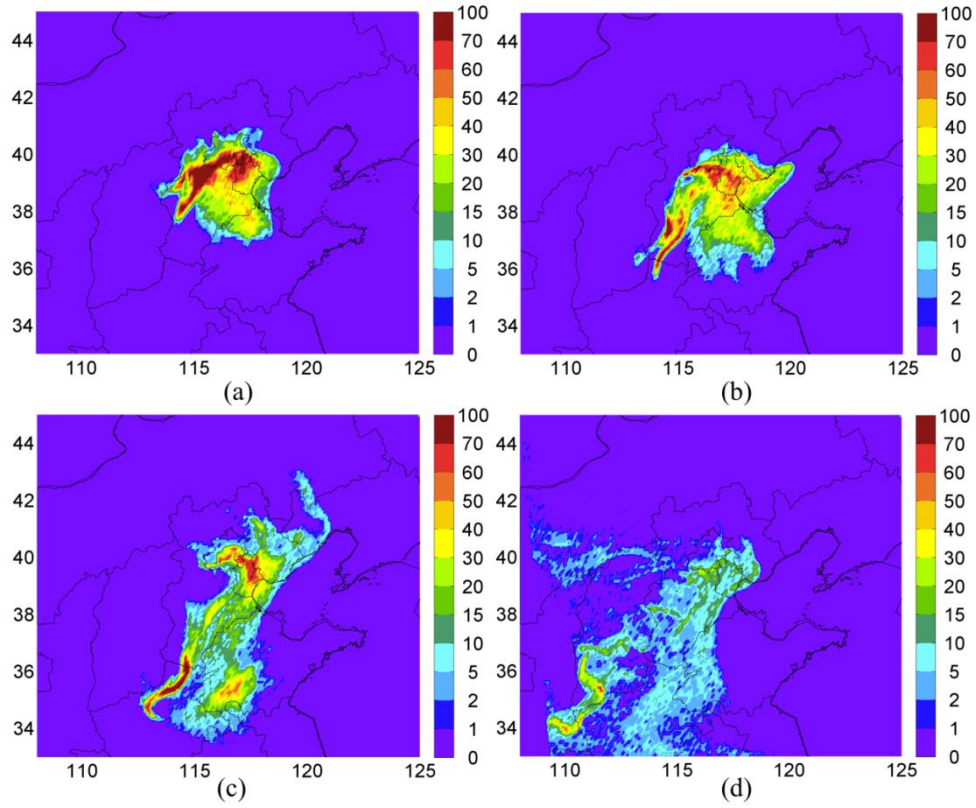


Figure 11. Observed (a) and simulated (b) chemical species of PM_{2.5} and simulated SOA (c) in the Beijing site

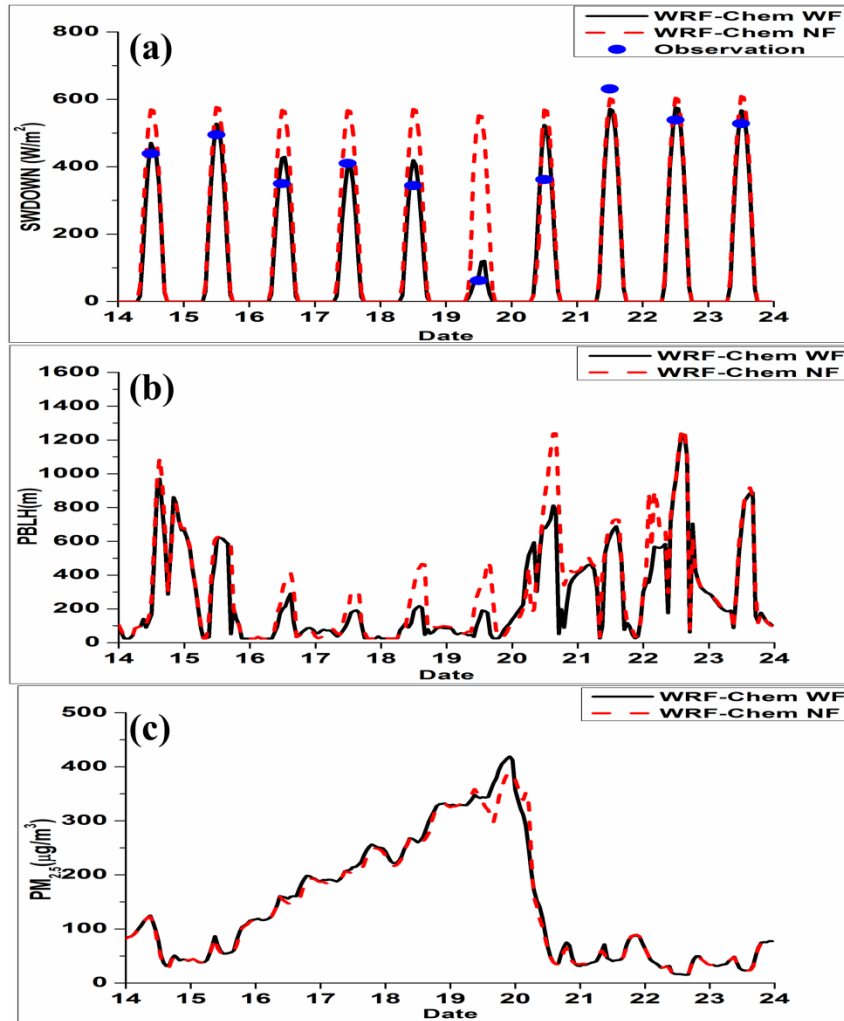
1
2
3
4
5
6
7

1



2

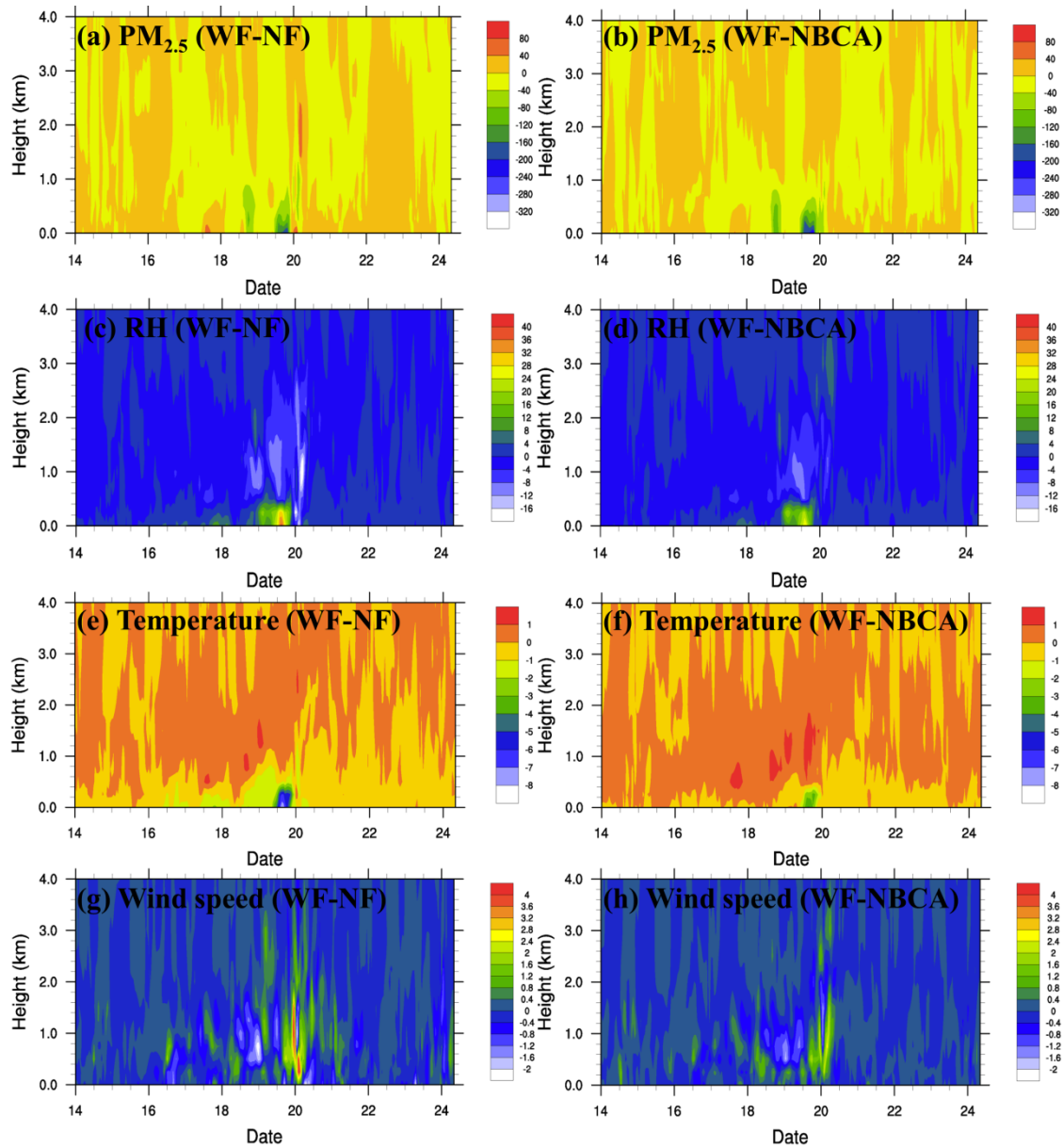
3 Figure 12. Backward dispersion of particles released on January 19 00:00, plotted 6, 12, 24, and
4 48 hours before being released (unit: number/grid cell)



1

2 Figure 13. Observed daily maximum surface solar radiation and simulated surface shortwave
 3 radiation for the with feedback (WF) and without feedback (NF) scenarios in Beijing (a),
 4 simulated PBLH (b) in WF and NF scenarios at Shijiazhuang, and simulated PM_{2.5} concentration
 5 (c) in WF and NF scenarios at Shijiazhuang

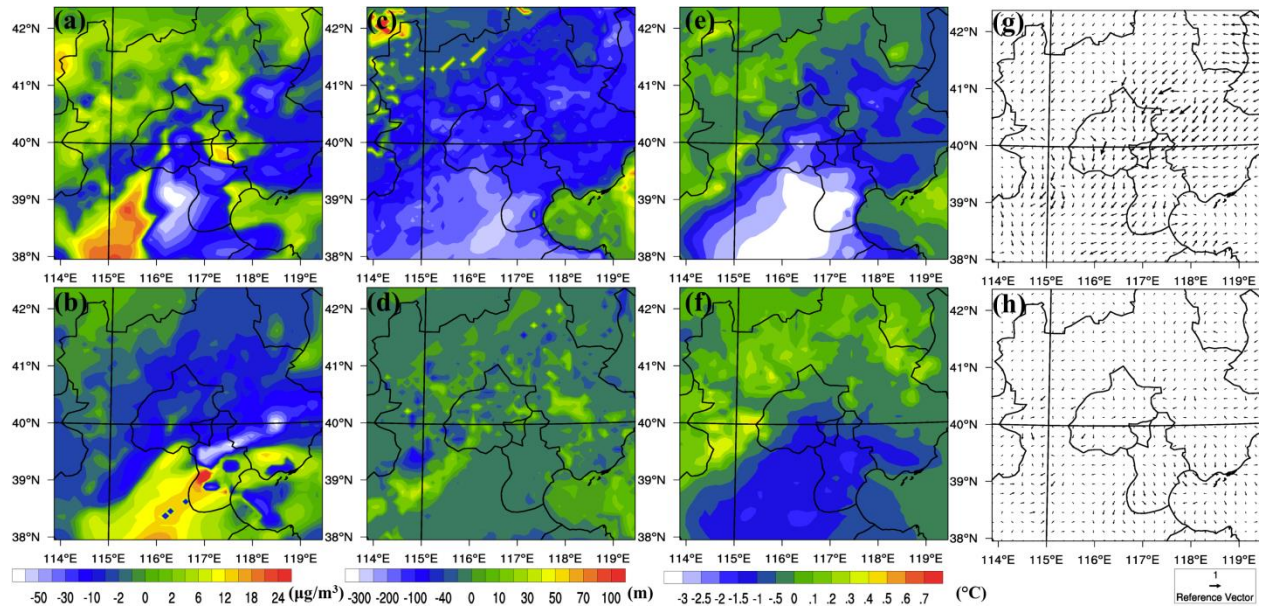
6



1

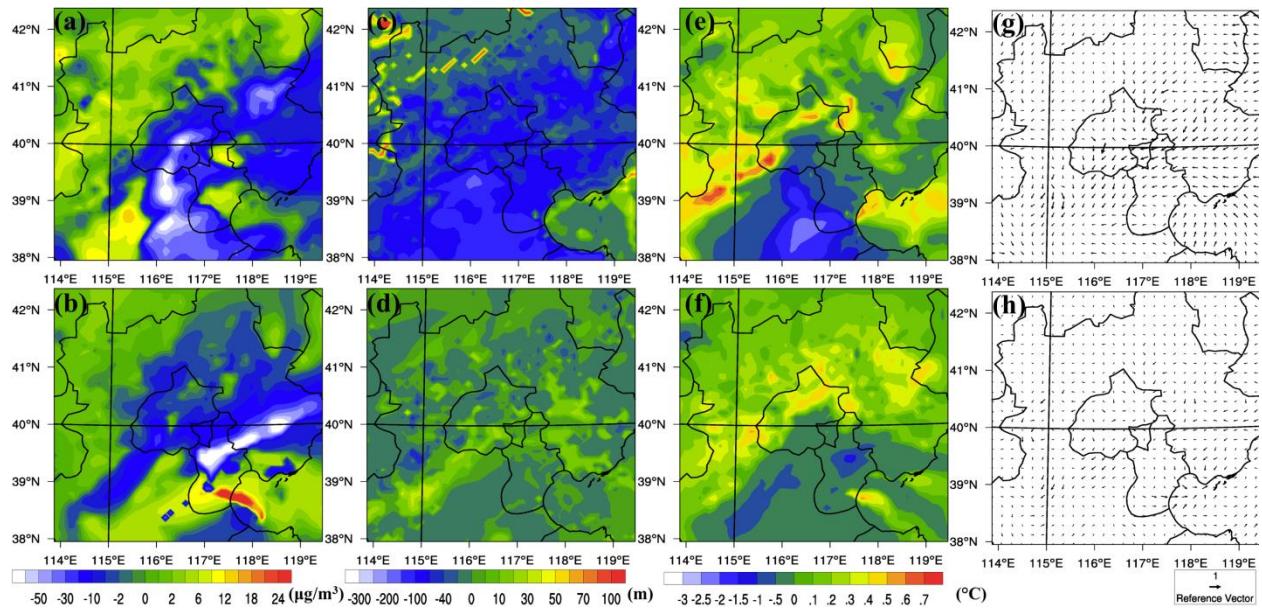
2 Figure 14. Temporal variations of vertical profiles of (a) PM_{2.5} (unit: μg/m³) (c) RH (unit: %) (e)
 3 temperature (unit: °C) (g) wind speeds (unit: m/s) differences in Beijing between WF and NF
 4 scenarios; (b), (d), (f) and (h) are PM_{2.5}, RH, temperature and wind speeds differences in Beijing
 5 between WF and NBCA (BC absorptions are teased out) scenarios

6



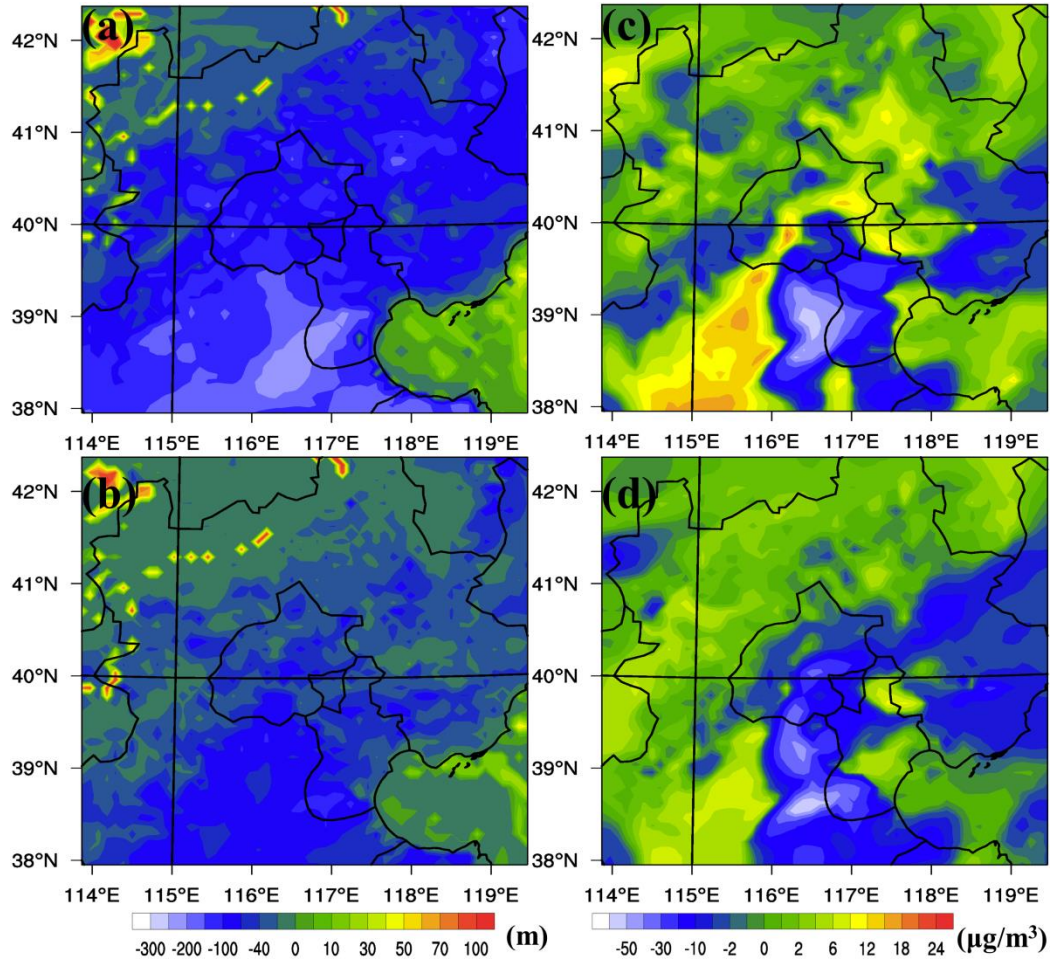
1
 2 Figure 15. Differences of PM_{2.5} concentration (unit: $\mu\text{g}/\text{m}^3$), temperature (unit: $^{\circ}\text{C}$), PBLH (unit:
 3 m) and horizontal wind (unit: m/s) at 2p.m. (a, c, e, g) and 2a.m. (b, d, f, h) between WF and NF
 4 scenarios

5



6
 7 Figure 16. Differences of PM_{2.5} concentration (unit: $\mu\text{g}/\text{m}^3$), temperature (unit: $^{\circ}\text{C}$), PBLH (unit:
 8 m) and horizontal wind (unit: m/s) at 2p.m. (a, c, e, g) and 2a.m. (b, d, f, h) between WF and
 9 NBCA scenarios

1



2

3

4

5

6

7

8

Figure 17. Differences of PBLH (unit: m) and PM_{2.5} concentration (unit: μg/m³) at 2p.m. between WF and NF scenarios (a, c) when BC emissions were reduced by half; differences of PBLH (unit: m) and PM_{2.5} concentration (unit: μg/m³) at 2p.m. between WF and NF scenarios (b, d) when BC emissions were reduced by half